2014

Fastener-Based Computational Models of Cold-Formed Steel Shear Walls

Thet Hein Tun
Bucknell University, tht001@bucknell.edu

Follow this and additional works at: https://digitalcommons.bucknell.edu/honors_theses

FASTENER-BASED COMPUTATIONAL MODELS OF

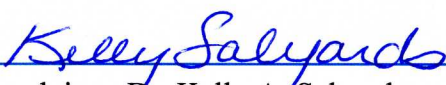# COLD-FORMED STEEL SHEAR WALLS

By

Thet Hein Tun

A Thesis Submitted to the Honors Council

For Honors in Civil and Environmental Engineering

April 10, 2014

Approved By:

Adviser: Dr. Stephen G. Buonopane

Co-adviser: Dr. Kelly A. Salyards

ACKNOWLEDGEMENTS

CONTENTS

LIST OF TABLES

LIST OF FIGURES

ABSTRACT

Cold-formed steel (CFS) combined with wood sheathing, such as oriented strand board (OSB), forms shear walls that can provide lateral resistance to seismic forces. The ability to accurately predict building deformations in damaged states under seismic excitations is a must for modern performance-based seismic design. However, few static or dynamic tests have been conducted on the non-linear behavior of CFS shear walls. Thus, the purpose of this research work is to provide and demonstrate a fastener-based computational model of CFS wall models that incorporates essential nonlinearities that may eventually lead to improvement of the current seismic design requirements. The approach is based on the understanding that complex interaction of the fasteners with the sheathing is an important factor in the non-linear behavior of the shear wall. The computational model consists of beam-column elements for the CFS framing and a rigid diaphragm for the sheathing. The framing and sheathing are connected with non-linear zero-length fastener elements to capture the OSB sheathing damage surrounding the fastener area. Employing computational programs such as OpenSees and MATLAB, 4 *ft.* x 9 *ft.*, 8 *ft.* x 9 *ft.* and 12 *ft.* x 9 *ft.* shear wall models are created, and monotonic lateral forces are applied to the computer models. The output data are then compared and analyzed with the available results of physical testing. The results indicate that the OpenSees model can accurately capture the initial stiffness, strength and non-linear behavior of the shear walls.

CHAPTER 1

1   INTRODUCTION

Lightweight cold-formed steel (CFS) is an effective construction material that is widely used for low and mid-rise buildings. CFS studs combined with wood sheathing, such as oriented strand board (OSB), form shear walls that provide lateral resistance to seismic forces. Modern performance-based seismic design relies on the ability to accurately predict building performance due to seismic excitations, and yet much remains to be understood regarding the CFS framing. Current standard design of multi-story CFS structures involves simplifications with regard to the non-linear inelastic behaviors derived from pure empirical tests. In addition, the displacement of the CFS framing system could involve the rotation of the framing system due to the asymmetric stiffness of the structure. Consequently, a more thorough study of CFS walls that includes more of the significant sources of nonlinearity is needed to provide knowledge for the development of modern seismic design requirements.

1.1   Objective

The research is part of a four-year Network for Earthquake Engineering Simulation (NEES) project, "Enabling Performance-Based Seismic Design of Multi-Story Cold-Formed Steel Structures" centered at Johns Hopkins University and funded by the National Science Foundation.

1.2   Scope and Thesis Statement

The computational modeling which forms the basis of this thesis relies on existing experimental results conducted as part of the CFS-NEES project. In order to characterize the hysteretic behavior of the connection between CFS frame members and sheathing when subjected to in-plane lateral forces, a series of experiments were conducted at Johns Hopkins University (JHU), as part of the CFS-NEES project. The hysteretic response from JHU's fastener tests is used as an input for computational modeling of the shear walls. In addition, full-scale CFS shear walls specifically designed for a two-story ledger-framed building underwent cyclic testing in a structural lab at the University of North Texas (UNT).

The scope of the thesis research is to create a refined numerical model of cold-formed steel shear walls that better represents physical behavior observed in tests when various lateral forces are applied to the model. While the results of the physical testing from the UNT shake table testing are used to validate the computational model, only a limited number of a combination of variable parameters can be tested in the laboratory. In addition, the outputs from numerical simulation can provide more detailed insights of the response of the CFS shear walls than the physical testing.

CHAPTER 2

2   LITERATURE SURVEY

2.1   Wood Framed Shear Walls

Physical testing in combination with advanced computational modeling provides insight on the non-linear performance of the shear walls. Literature on wood framed, sheathed shear walls provides understanding of force-displacement behavior of individual fasteners, which is fundamental to the simulation of the CFS model detailed in this thesis. Previous models include numerical model of non-linear response of wood frame shear wall under static lateral loads and earthquake excitations (Filiatrault, 1990), and under arbitrary quasi-cyclic loading (Folz and Filiatrault, 2001).

Wood framed shear wall assemblies are typically composed of four basic structural components: framing members (plate, studs and sill), sheathing panels, sheathing-to-framing connectors, and hold-down anchorage devices (Figure 1). Filiatrault (1990) formulates a numerical model of the non-linear response of wood frame shear wall models configured from different numbers of rectangular sheathing panels of different sizes and frame-to-sheathing connectors (Figure 1). The two-dimensional model predicts the lateral stiffness and the ultimate lateral load carrying capacity of shear walls under static lateral loads, and the dynamic response under specified earthquake ground motion. The model assumes pin-connected, rigid frame members. Thus, when lateral loads are applied, the frames distort into a parallelogram

with the top and bottom plates remaining horizontal. The sheathing panels, on the other hand, develop in-plane shear deformations along with rigid-body translations and rotations (Figure 2). To verify the accuracy of the computational model, the results are compared to static unidirectional, free-vibration and shake table tests. The main source of energy dissipation in wood frame shear walls results from the frame-to-sheathing connectors through hysteresis.
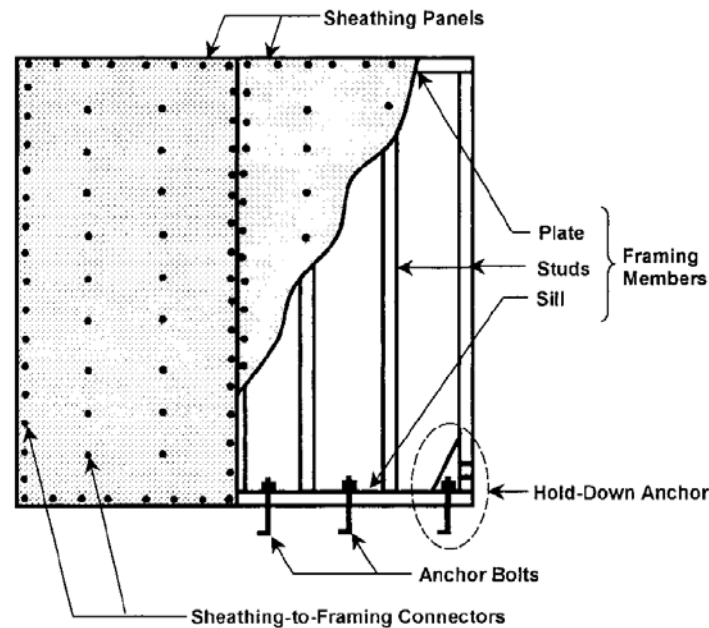
Figure 1. Basic structural configuration of a wood frame shear wall (Folz, Filiatrault, 2001).

4

Figure 2. Distortion of sheathing panel and framing members of a wood frame shear wall under lateral load (Filiatrault, 1990).

Similarly, testing and research on wood sheathed shear walls, explored by Folz and Filiatrault (2001), reveal that the complex interaction between individual fasteners and the sheathing is an important factor in understanding the non-linear behavior of the shear wall as whole. Because of the relative motion between the sheathing and framing, the fasteners gradually damage the sheathing material, thereby creating non-linear response.

Folz and Filiatrault (2004a) develop a single non-linear shear element that can reproduce the response of a full wood frame shear wall. The shear wall elements are then used to create a model of a building with multiple shear walls and rigid floor diaphragms. Although their research work is beyond the scope of the current research but indicates a possible future application of how the current fastener-based computational modeling can be used to model an entire building.

Folz and Filiatrault (2004a) present the formulation of a numerical model that predicts the dynamic characteristics, quasi-static pushover and seismic response of light-frame wood buildings. The building structure of the model is comprised of two primary components: rigid horizontal diaphragms and nonlinear lateral load resisting shear wall elements. The two-dimensional planar model is obtained by rendering the walls of the actual three-dimensional building with equivalent zero-height shear wall spring elements (Figure 3). The non-linear spring elements then interconnect the diaphragms or tie the structure to rigid foundations. In order to calibrate the properties of the shear wall spring elements, accurate findings of the strength and stiffness degrading hysteretic characteristics of the shear wall are necessary. Determining the hysteretic characteristics from the shear wall responses is crucial in developing CFS computational models. The response of the building is subsequently defined in terms of only three degrees of freedom per floor. Folz and Filiatrault (2004b) present the model results from full-scale shake table tests of the two-story wood-frame building.
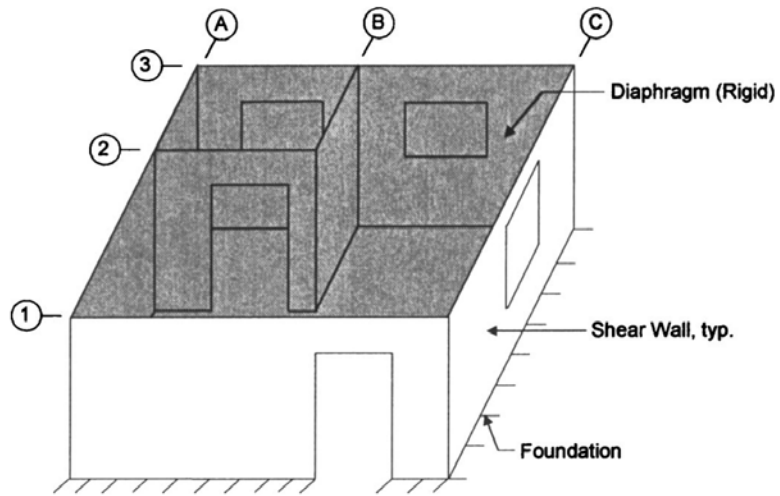
(a)
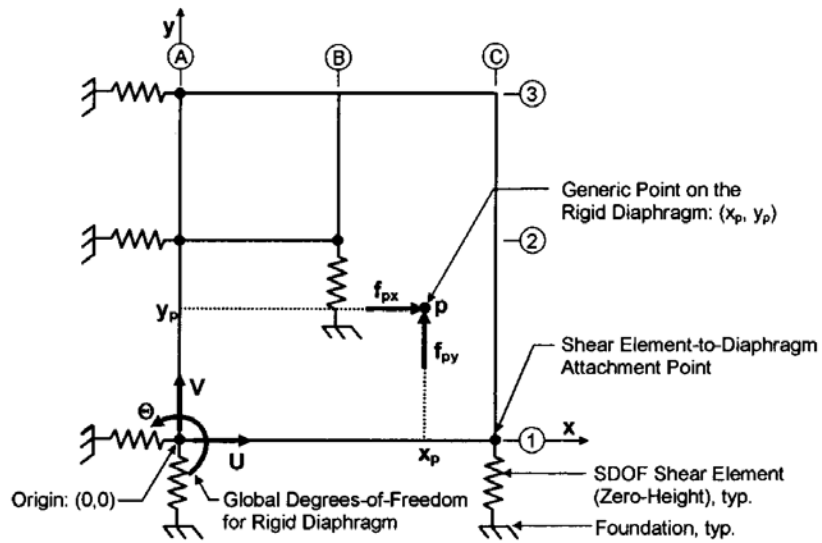
(b)

Figure 3. (a) Three-dimensional model of single-story wood frame structure; (b) Two-dimensional planar model of the same single-story wood frame structure (Filiatrault, 2004).

2.2   Cold-Formed Steel Framed Shear walls

Xu and Martinez (2006) presents an analytical method that employs an iterative procedure to evaluate the ultimate lateral strength and displacement of a cold-formed steel shear wall with sheathing. The method takes into consideration the effects of material property, thickness and geometry of sheathing and studs, spacing of studs, and geometric arrangement of fasteners and framing members. The paper incorporates test results derived from various fastener configurations from full-scale shear walls in order to calibrate complex spring elements. Compared to this approach, our computational approach allows us to investigate many more possible shear wall configurations and thus to understand much more complex nature of the behavior of the shear walls without modeling an entire building. In scenarios where experimental data is not readily available for simple shear wall models, the analytical approach of Xu and Martinez (2006) can provide quick practical estimates.

Celik and Engleder (2010) develop a semi-analytical model to calculate the shear strength of cold-formed steel framed shear walls. The concept of the analytical model was grounded on the understanding that the resulting shear resistance of the sheathed wall can be calculated as the sum of individual fastener resistances. The physical tests were based on several full-scale shear wall assemblies and shear load performance of individual fasteners which connect plywood to cold-formed steel members. The tests observed plywood pull-over failure at the bottom corners. Similar behavior is observed in this thesis using the fastener-based computational analysis approach. Employing

statistical methods such as least square fitting, the physical testing results were subsequently incorporated into the analytical model.

Fiorino, et al. (2006) proposes an analytical approach to predict the non-linear shear vs. top wall displacement relationship of sheathed cold-formed shear walls under nonlinear earthquake excitation. The research's method relies on the available screw connection test results. The analytical results, when compared to experiments, reveal that the prediction of wall deflection is not as accurate as the strength prediction. In addition, since the analytical method is based on limited experimental data on connections and walls, the outcomes from proposed approach can only be considered as preliminary results for actual implementation.

Fülöp and Dubina (2004) conducted a full-scale shear wall test on different wall panels and parameters that influence the earthquake behavior of the light thin-walled load bearing structures. From the paper's experimental results, the wall panels display significant shear-resistance in terms of rigidity and load bearing capacity to effectively resist lateral loads. Moreover, hysteretic behavior is characterized by significant pinching that reduces energy dissipation. The experiments also reveal that failure starts at the bottom track in the anchor bolt region. Thus, the authors conclude that the strength of the corner detail is critical since it can subsequently have effects on the initial rigidity of the wall system. This loss of rigidity, in turn, can cause large sway and premature failure of the panel. These findings can be applicable for the modeling of the anchors to the bottom track in our research in order to avoid premature failure of the panel wall.

Fiorino, et al. (2012) presents the results of an extensive parametric non-linear dynamic analysis carried out on one story buildings with sheathed cold-formed steel structural systems. The research considers wall configurations and investigates parameters such as sheathing panel, wall geometry, external screw spacing, seismic weight and soil type. The analysis is performed using incremental dynamic analysis (IDA) by applying an ad hoc model of the hysteretic response of the shear walls. This IDA approach to studying the shear walls hysteresis is one of the main methods employed in examining the sheathed cold-formed steel structure systems. Similar to our research, this paper is based on the premise that the seismic behavior of shear walls is strongly influenced by the sheathing-to-frame connections response, which is characterized by non-linear and hysteretic pinching response.

The purpose of the research conducted by Della Corte et al. (2006) was to investigate whether sheathed cold-formed steel structures can survive more violent earthquakes which exceed the design intensity. The researchers claim that cold-formed structures, if adequately designed, could be less vulnerable to seismic damage than other ordinary structures. According to modern design standards, design basis earthquakes are typically defined as earthquakes with a 10% probability of being exceeded in 50 years. The numerical modeling of cold-formed shear walls takes into account two major characteristics of the sheathed walls: strong nonlinearity of lateral load-displacement relationship, and strong pinching of hysteresis loops. The conclusion from the research was that sheathed steel stud walls can be designed to meet enhanced seismic standards in low and medium seismic intensity zones. Based on the non-linear responses predicted

from our computational model, future application may include improving current seismic design codes for CFS shear wall structures.

2.3   AISI S213 Code

American Iron and Steel Institute (AISI) classifies shear walls as either Type I shear walls or Type II shear walls. For Type I shear walls, hold-downs are located at the end of each shear wall "segment" whereas Type II only has two hold-downs, one at each end of the wall (Figure 4). The present computational research employs Type I shear walls.

(a)

(b)
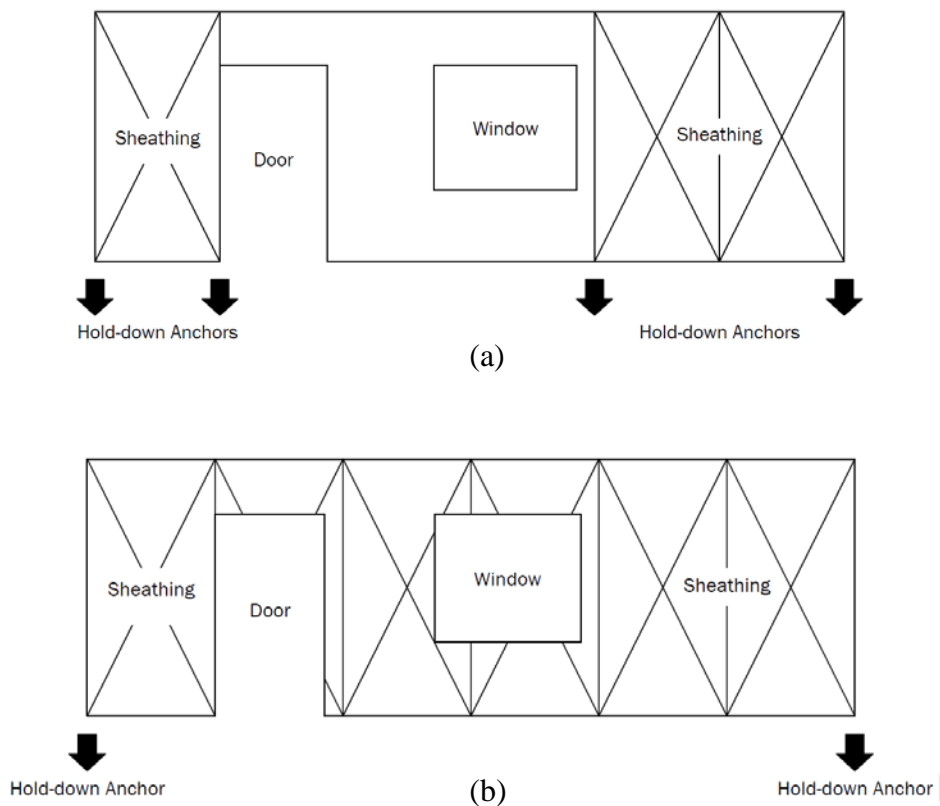
Figure 4. Classification of shear walls: (a) Typical *Type I* Shear Wall, (b) Typical Type II Shear Wall (AISI, 2007).

The strength and lateral deflection requirements for Type I shear walls in AISI S213-07 were based on a series of investigations by Serrette (1996, 1997, 2002, 2003). The available strength or factored resistance for a chosen assembly (in this case 7/16" OSB sheathing wall) can be determined by using the nominal strength and dividing or multiplying the appropriate safety factor (Ω) and resistance factor (ϕ), respectively (Table 1).

Table 1. Nominal shear strength (R_n), safety factor (Ω) and resistance factor (ϕ) for seismic loads for 7/16" OSB shear walls with given specifications

Assembly Description	7/16" OSB, one side
Max. Aspect Ratio (h/w)	2:1
Fastener Spacing at Panel Edges (inches)	6
Designation Thickness of Stud, Track and Blocking (mils)	54
Required Sheathing Screw Size	8
Required nominal Shear Strength (R_n) (pounds per foot)	940
Safety factor (Ω) (for ASD)	2.50
Resistance factor (ϕ) (for LRFD – seismic)	0.60
Resistance factor (ϕ) (for LSD – gypsum sheathed walls)	0.60

At the design strength, the lateral deflections of the computational shear wall model are predicted. Equation C2.1-1 of AISI S213-07 provides calculation of the lateral deflection of cold-formed steel light-framed shear walls (AISI, 2007):

$$\delta = \frac{8vh^3}{E_s A_c b} + \omega_1 \omega_2 \frac{vh}{\rho G t_{sheathing}} + \omega_1^{5/4} \omega_2 \omega_3 \omega_4 \left(\frac{v}{\beta}\right)^2 + \frac{h}{b}\delta_v \qquad \text{Eq (1)}$$

where,

A_C =   gross cross-sectional area of chord member (in^2)

b =   width of the shear wall (ft.)

E_s =   modulus of elasticity of steel (= 29,500,000 psi)

G =   shear modulus of sheathing material (psi)

h =   wall height (ft.)

s =   maximum fastener spacing at panel edges (in)

$t_{sheathing}$=   nominal panel thickness (in)

v =   shear demand (V/b) (lb. per linear foot)

V =   total lateral load applied to the shear wall (lb.)

β =   660 (for OSB)

δ =   calculated deflection (in)

δ_v = vertical deformation of anchorage/ attachment details (in)

ρ = 1.05 for OSB

ω_1 = $s/6$

ω_2 = $0.033/t_{stud}$ (t_{stud} = framing designation thickness in inches)

ω_3 = $\sqrt{0.5h/b}$

ω_4 = 1 (for wood structural panels)

In order to account for inelastic behavior and effective shear in the sheathing material, the equation uses simple mechanics-based models for the shear wall behavior and incorporates empirical factors. The empirical factors are based on regression and interpolation analyses of reversed cyclic test data employed in the development of the International Building Code (IBC) CFS shear design values (Serrette and Chau, 2003). The equation contains four additive terms, associated with primary contributions of the lateral deflection of the shear wall (Figure 5): linear elastic cantilever bending (first term from Eq. 1), linear shear deformation of sheathing (second term), overall non-linear effects (third term), and overturning due to hold-down extension (final term).
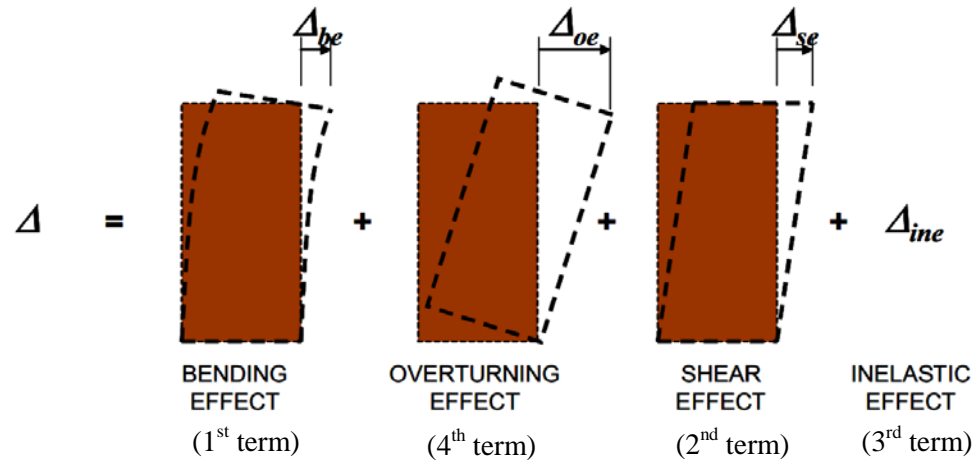
Figure 5. Modeling of total lateral deflection (Serrette and Chau, 2003).

The terms for cantilever bending and hold-down deformations are derived from the fundamentals of mechanics. The term for shear deformation is the product of the expression for elastic in-plane shear deformation and empirical adjustment factors (ρ, ω_1 and ω_2). The ρ term accounts for observed differences in the response of walls with different sheathing materials. The non-linear deflection term, Δ_{ine} that accounts for inelastic effect is purely empirical and is developed by comparing envelope results from regression analyses of the above-mentioned cyclic tests. The lateral contribution from the fourth term depends on the height to width ratio of the shear wall and the axial stiffness of the hold-down.

When each term of the lateral deflection is graphed up to a lateral strength of 9,900 lb. for a 12 *ft.* width wall using S213 Equation (Figure 6), the non-linear term, Δ_{ine} contributes significantly to the total deflection. The combination of the rest of the three

terms, which can be mainly derived from mechanics, contributes less than 50% of the total deflection. Since Δ_{ine} is a purely empirical term, little is known about what this term actually entails. The fastener-based computational approach in this research seeks to measure and explain this non-linear response and provide a better tool for its prediction.
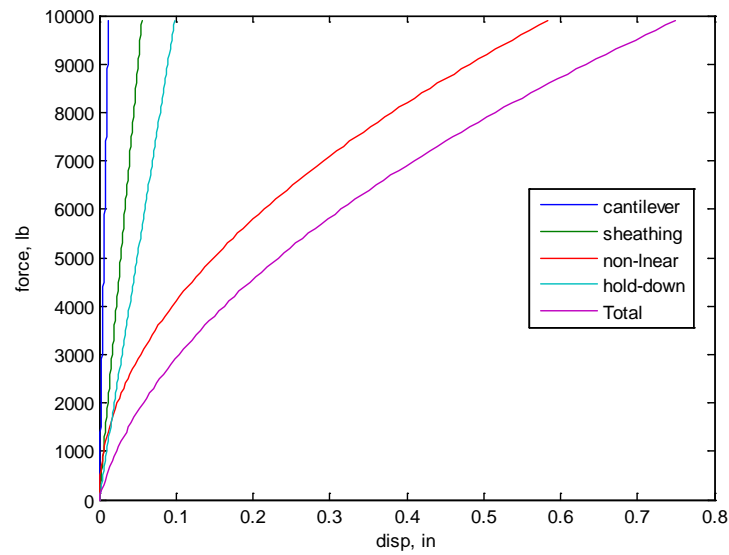
Figure 6. The effects of various deflection terms up to lateral strength (9900 lb.) for a 12 *ft.* width wall based on Eq. C2.1-1 of AISI 213-07.

CHAPTER 3

3 DEVELOPMENT OF THE COMPUTATION MODEL

This research employs the OpenSees (Open System for Earthquake Engineering Simulation) structural analysis software in order to create a fastener-based computational model of CFS shear walls with sheathing. OpenSees is an object-oriented, open source software framework that can create parallel finite element computer applications for simulating the performance of structural and geotechnical systems subjected to earthquakes (McKenna et al., 2011). Because it is a general purpose non-linear dynamic analysis software, OpenSees permits modeling flexibility and has the capability to incorporate multiple shear walls or a full building. While OpenSees is employed to perform finite element analysis to obtain the seismic response data, MATLAB is used to define the physical configurations of the shear wall models and post-process the results.

3.1 Physical Testing of Shear Walls

Full-scale CFS shear walls specifically designed for a two-story ledger-framed building underwent monotonic and cyclic tests in a structural lab at University of North Texas and details of the tests can be found in Liu et al. (2012). The physical tests examined the effects of geometry (varying widths of 4 *ft.* and 8 *ft.*), sheathing types (OSB and gypsum), location of sheathing seam(s), and, presence of the framing ledger

on the nonlinear response. The general construction of the shear walls are detailed in

Figure 7 and the key features considered in the computational model are boxed in red.

<div align="center">(a) front view   (b) back view</div>
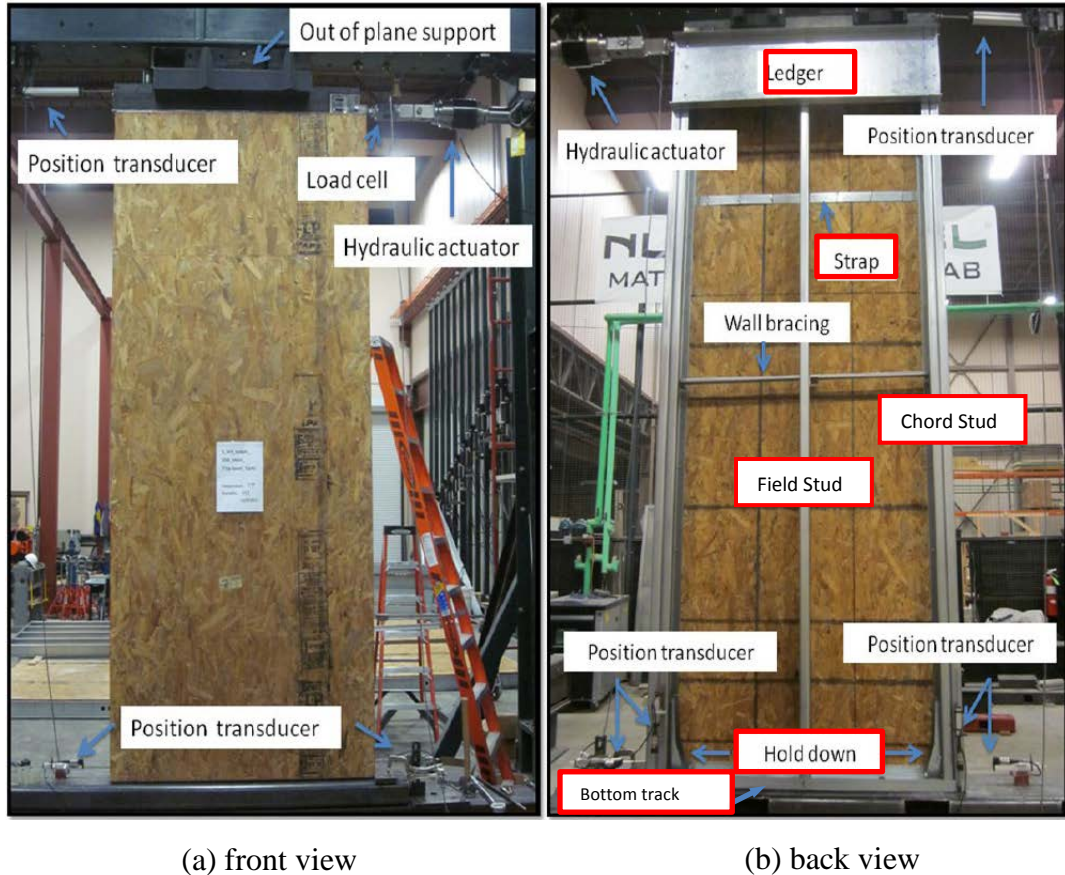
Figure 7. Test setup and specimen details (Liu et al., 2012).

The basic geometries of 4 *ft*. x 9 *ft*. or 8 *ft*. x 9 *ft*. walls, framed with vertical studs,

are spaced 24 inches apart. The vertical studs were connected to the horizontal tracks

with No. 10 flathead screws. The exterior or chord studs are back-to-back double studs

and the interior or fixed studs are single studs. The studs and tracks are 600S162-54 and

600T150-54, respectively with both having yield strength of 50 *ksi*. The cold-formed

<div align="center">18</div>

steel has a modulus of elasticity of 29,500 *ksi* and a shear modulus of 11,200 *ksi*. The ledger is a 1200T200-097 section with yield strength of 50 *ksi*, and is attached to the top 1 *ft.* of the interior face of the CFS wall using No. 10 flathead screws. The following table (Table 2) shows the section properties of studs, tracks and ledgers used in the physical tests and computational models.

Table 2. Section properties of CFS studs, tracks and ledger

Properties	*Double stud* (2 x 600S162-54)	*Single stud* (600S162-54)	*Top track* (600T150-54)	*Bottom track* (600T150-54)	*Ledger* (1200T200-097)
Area (*in.*^{2})	2×0.556	0.556	0.509	0.509	1.63
Moment of inertia (strong axis) (*in.*^{4})	2×2.86	2.86	2.61	2.61	29.8
Moment of inertia (weak axis) (*in.*^{4})	1.0244	0.329	0.0907	0.0907	0.41
Torsional inertia (*in.*^{4})	2×5.94×10^{-4}	5.94×10^{-4}	5.43×10^{-4}	5.43×10^{-4}	5.60×10^{-3}

The physical tests used No. 8 flathead screws (1-15/16 *in.* long) to fasten the 7/16 *in.* thick orientated strand board (OSB) sheathing to the studs and tracks. The OSB type was 24/16, exposure 1 rated. On the perimeter of the sheathing, the screws were spaced at 6 *in.*, and along the interior studs, the screws were spaced at 12 *in.* (Figure 8). CFS construction contains horizontal and vertical seams in the OSB sheathing because the sheathing is commonly manufactured in 4 *ft.* x 8 *ft.* sheets. Vertical seams are supported at interior stud location at every 4 *ft.* width. Horizontal seams are bridged with a 1.5 *in.* wide 54 *mil* steel seam strap.
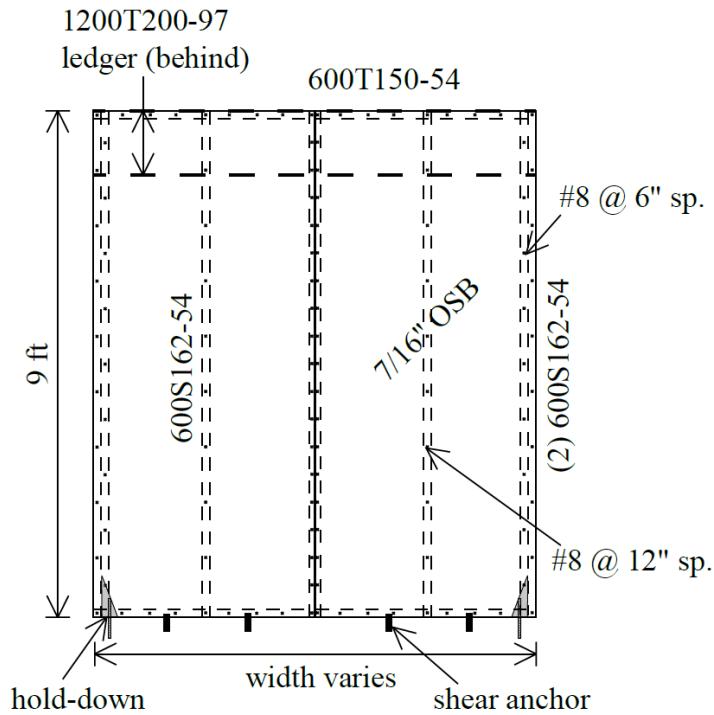
Figure 8. Typical CFS shear wall configuration (Buonopane et al., 2014).

Simpson StrongTie® S/HDU6 hold-downs with No.14 HWT self-drilling screws were installed at the exterior chord studs. The hold-downs were connected to the steel base using 5/8 *in.* diameter 2.5 *in.* long ASTM 325 anchor bolts. In addition, the bottom track of the shear walls were bolted to the steel testing frame with 5/8 *in.* anchor bolts at 24 *in.* on-center along the wall with standard washers and nuts. In typical CFS construction, the shear anchors would consist of low-velocity fasteners anchored into the foundation material. Four bolts were used for 4 *ft.* x 9 *ft.* shear walls and six bolts for 8 *ft.* x 9 *ft.* shear walls (Figure 9).
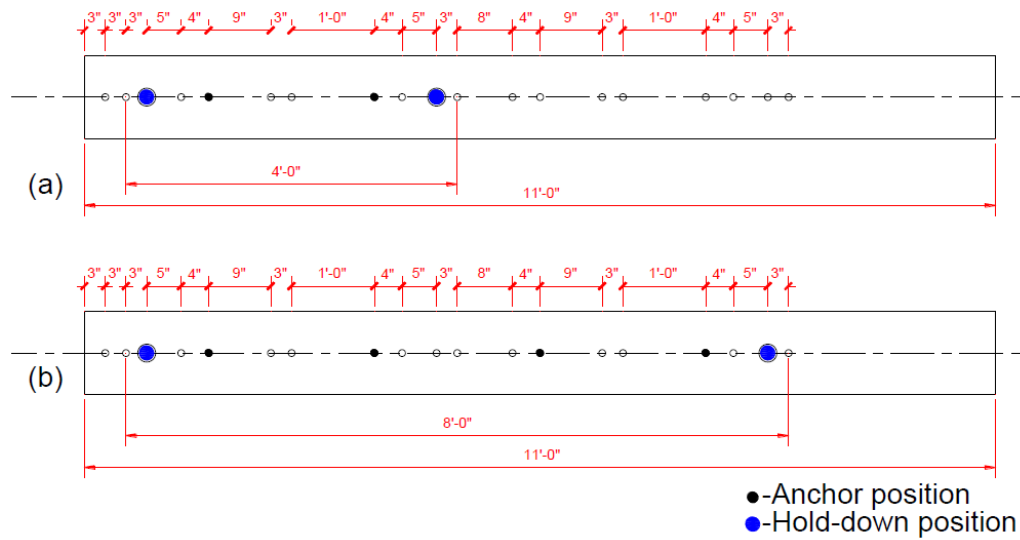
Figure 9. Hold-down and anchor placements along frame base (top view) for: (a) 4 *ft.* and (b) 8 *ft.* wide wall (Liu et al., 2012).

Monotonic and cyclic tests were performed in displacement control, following ASTM E564 (2006). According to the test results, specimens generally failed at perimeter and corner sheathing-to-stud fastener locations. The most common failure modes were a pull-through or bearing failure. Figure 10 illustrates all observed fastener failure modes and Figure 11 displays the force-displacement response of a typical shear wall, along with key response results.
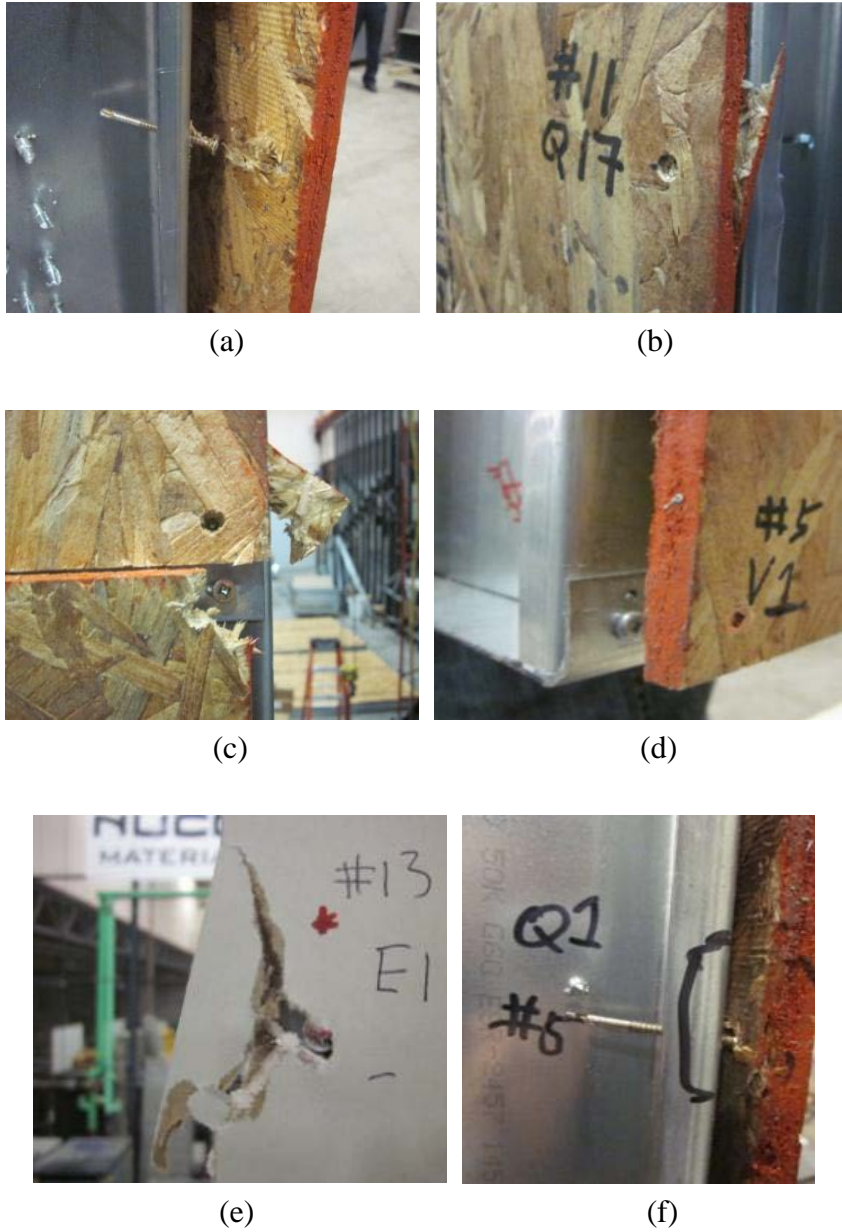
Figure 10. Observed fastener-sheathing modes of failure: (a) pull-through, (b) wood bearing failure, (c) tear out of sheathing, (d) cut off head (screw shear), (e) enlarged hole, (f) partial pull through (Liu et al., 2012).

Test results

Maximum +load: 1160plf

Maximum +load: 4640lbf

Net lateral displacement at top of wall at Maximum +load: 2.917in.

Maximum -load: -1044plf

Maximum -load: -4179lbs

Net lateral displacement at top of wall at Maximum -load: -2.714 in.

Average maximum load: 1102plf

Average net displacement: 2.815in.
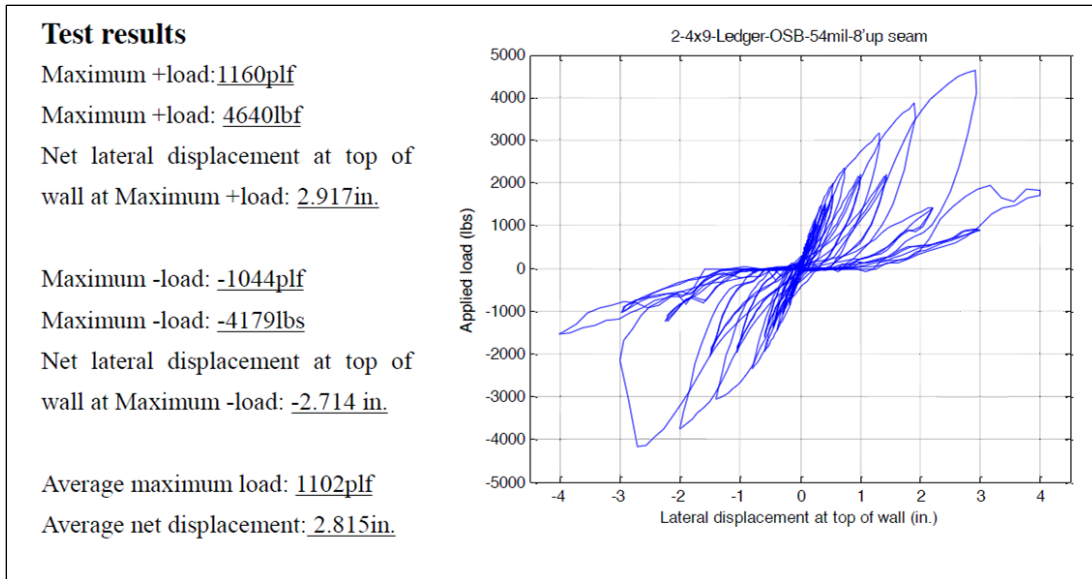
Figure 11. Force-displacement response for physical testing of a 4 *ft.* x 9 *ft.* wall (UNT test 2) (Liu et al., 2012).

3.2   Fastener Testing

The seismic performance of CFS structures relies on the non-linear behavior of its shear walls. This research examines the contribution of the individual fasteners to this nonlinearity. This is because, on one hand, the CFS members of a shear wall, having minimal lateral resistance, act as a hinged frame and deform in the shape of a parallelogram. On the other hand, the sheathing, due to its substantial in-plane rigidity, acts as a rigid body and remains in the shape of a rectangle. The deformation incompatibilities between the CFS framing and sheathing cause a displacement demand at the fastener connections, which is satisfied by a combination of fastener movement,

fastener deformation, and localized deformation and damage to the sheathing surrounding the individual fastener (Figure 12).
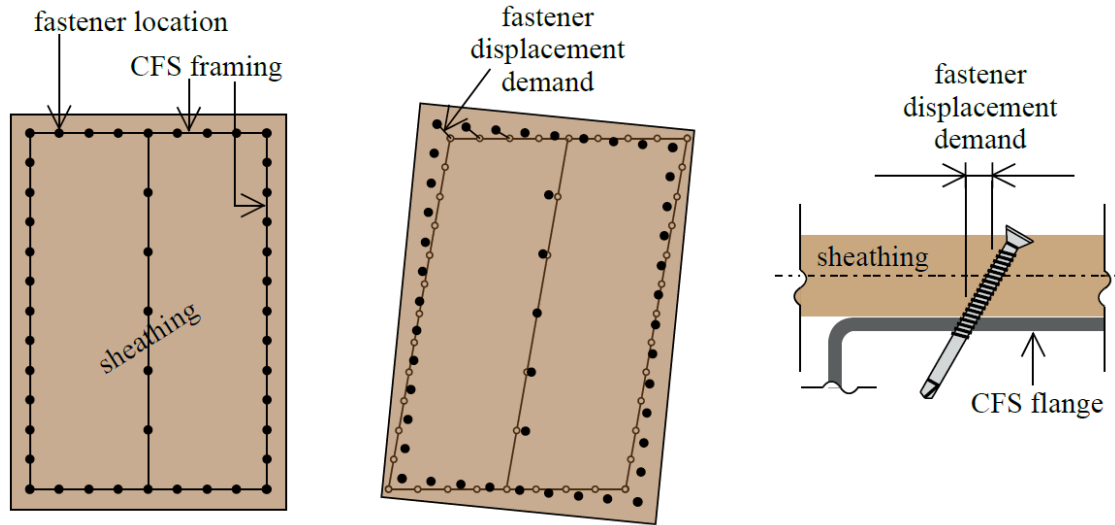
Figure 12. Display of fastener displacement demand: (a) Initial Configuration; (b) Deformed Configuration; (c) Deformed Cross-sectional Details (Buonopane et al., 2014).

The force-displacement behavior of the fastener connections is found to be greatly non-linear, displaying the characteristics of hysteresis, degradation and pinching (Section 2.2). The local behavior of each individual fastener collectively creates the non-linear force-deflection response of the CFS shear wall as a whole (Figure 12). There are several approaches to capture the non-linear behavior of the shear walls in computational models. One approach would be to calibrate complex shell or spring elements using test results from full-scale shear walls (Fülöp and Dubina, 2004). However, estimating non-linear properties is difficult if there are no companion test

results. The method employed in this research is to model the location and behavior of each fastener, with individual fastner behavior defined based on experimental results. The approach allows simplifying assumptions such as semi-rigid and flexible CFS members and the option to include hold-down flexibility. Using results from a series of experiments conducted at Johns Hopkins University (JHU), the researchers there characterized and normalized the force-displacement behavior occurring at individual fasteners.
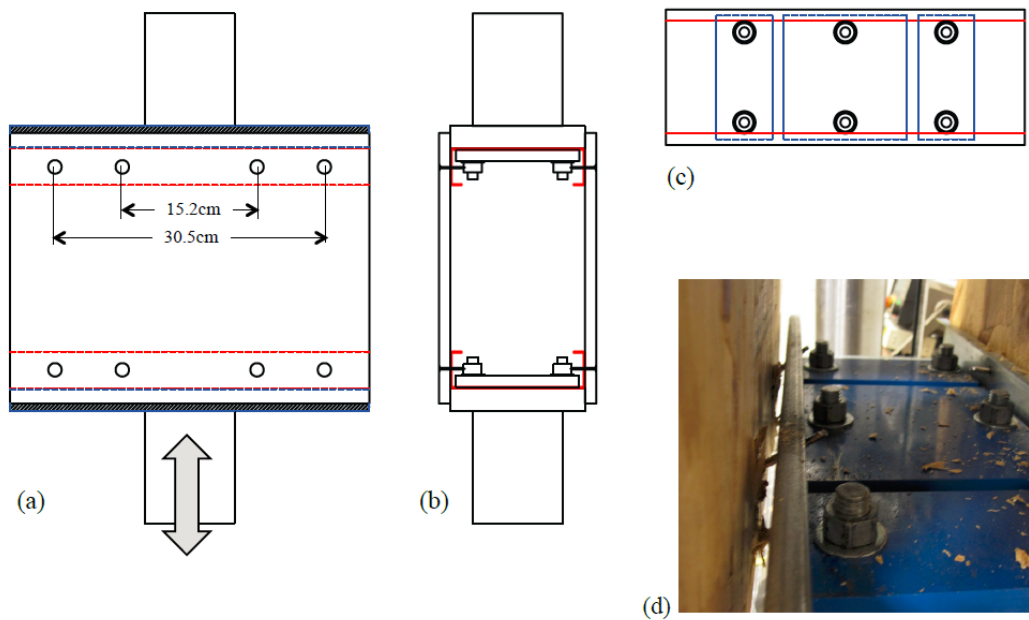
Figure 13. Photograph of general setup for fastener test using OSB (Peterman and Schafer, 2013).

The general set up of the testing rig and specimen, along with the details of fastener failure and damage, is shown in Figure 13. For all the tests, 6 inch deep cold-formed steel channel sections (600S162) were used. Three nominal steel thicknesses—

33, 54, and 97 mil—were tested. Two fastener spacings—6 inches and 12 inches to simulate typical spacings used in chord and field studs, respectively—were also tested. From monotonic tests, it was determined that the fastener spacings of either 6 or 12 inches do not significantly affect the strength of the connection between CFS and sheathing. In addition, the fastener stiffness <GIVE VALUE> from the monotonic tests is used as the fastener stiffness for the linear analysis models in OpenSees.

An example of cyclic test results is provided in Figure 14 for a specimen with 54 mil studs, OSB sheathing and 6 inch fastener spacing. The force-deformation response is greatly pinched with almost no force in the second and fourth quadrants of the force-deformation diagram.

(a)
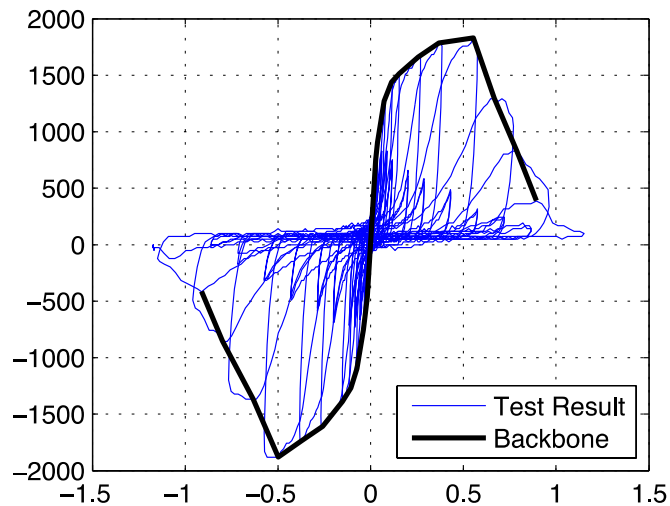
Figure 14. *Pinching4* **model and Backbone curve from 54** *mil* **steel with 6** *in.* **spacing (Peterman and Schafer, 2013).**

Hysteretic characterization of the stud-fastener-sheathing performance was accomplished by using the *Pinching4* material model, as implemented in OpenSees (Lowes, et al., 2004). As depicted in Figure 15, *Pinching4* parameters include four positive and four negative points that define the loading or backbone curve, and six additional parameters that define the unloading and re-loading behavior of the material.

pinching4
backbone

(ePd_1, ePf_1)
(ePd_2, ePf_2)
(ePd_3, ePf_3)
(ePd_4, ePf_4)
(eNd_1, eNf_1)
(eNd_2, eNf_2)
(eNd_3, eNf_3)
(eNd_4, eNf_4)

load
deformation

$a = (rDispP \cdot d_{max}, rForceP \cdot f(d_{max}))$
$b = (d_{max}, f(d_{max}))$
$c = (*, uForceN \cdot eNf_3)$
$d = (rDispN \cdot d_{min}, rForceN \cdot f(d_{min}))$
$e = (d_{min}, f(d_{min}))$
$f = (*, uForceP \cdot ePf_3)$
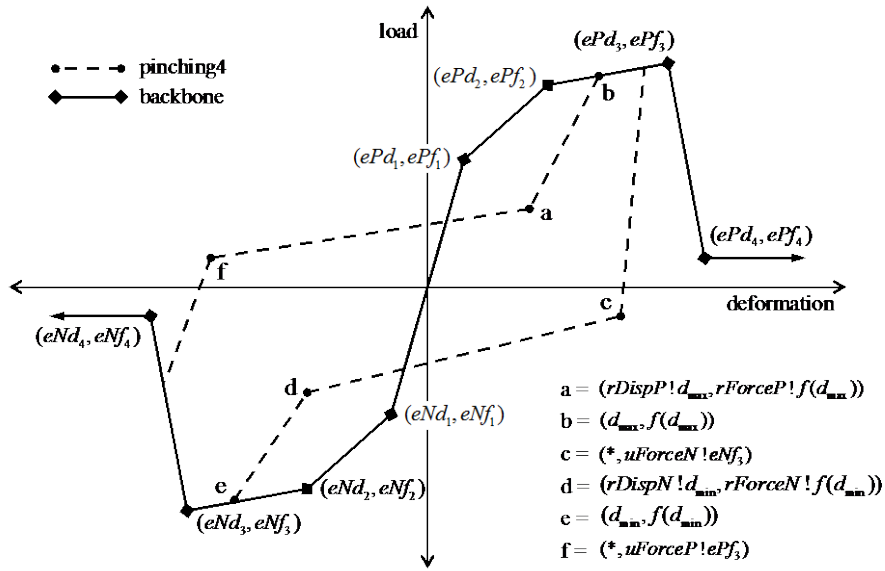
Figure 15. *Pinching4* hysteresis parameters (Lowes, et al., 2004).

Using the *Pinching4* model, the behavioral response of each individual fastener can be approximated computationally. An example of the fitted *Pinching4* model imposed on the actual test data is provided in Figure 16.

13−./testdata/c54o6_1.txt
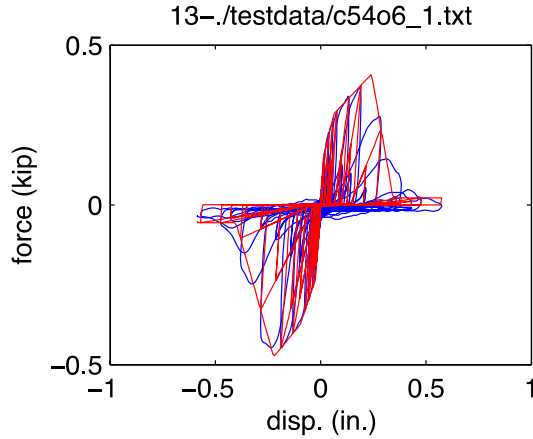
Figure 16. *Pinching4* **model imposed on actual test data (Peterman and Schafer, 2013).**

For computational modeling of the shear walls in the current research, the hysteretic response from overall fastener tests give in Table 3 is used as an input.

Table 3. Basic pinching4 model parameters for 54 *mil* **steel with OSB sheathing (per fastener values) (Peterman and Schafer, 2013).**

(a) Pinching4 Backbone points

eNd4 (in.)	eNd3 (in.)	eNd2 (in.)	eNd1 (in.)	ePd1(in.)	ePd2 (in.)	ePd3 (in.)	ePd4 (in.)	eNf4 (kip)	eNf3 (kip)	eNf2 (kip)	eNf1 (kip)	ePf1 (kip)	ePf2 (kip)	ePf3 (kip)	ePf4 (kip)
symmetric				.020	.078	.246	.414	symmetric				.22	.35	.46	.049

(b) Unloading and reloading Pinching4 parameters

rDispP	rForceP	uForceP	rDispN	rForceN	uForceN
0.42	0.01	0.001	Symmetric		

28

3.3 Development of the Computational Model

3.3.1 Test matrix

The computational modeling for this research combines the non-linear force-deformation relationship for individual fasteners with the overall geometry and structural properties of the sheathing and the CFS framing. In addition to the overall wall geometry and fastenter layout, the analyses focus on examining four specific modeling aspects: hold-downs, shear anchors, vertical seams and ledger track. Table 4 summarizes different model variations.

Table 4. Summary of OpenSees model variations with their respective initial linear stiffness and displacement at 1000 lb. lateral force

Analysis Name	Width (*ft.*)	Model Features			
		hold down	shear anchors	vertical seam	ledger as diaphragm
L4_1	4	pinned	none	n/a	no
L4_2	4	elastic	none	n/a	no
L4_3	4	elastic	pinned	n/a	no
L4_4	4	elastic	pinned	n/a	yes
L4_5	4	elastic	none	n/a	yes
L8_1	8	pinned	none	1	no
L8_2d	8	elastic	none	1	no
L8_3	8	elastic	pinned	1	no
L8_4	8	elastic	pinned	1	yes
L8_5d	8	elastic	none	1	yes
L8_2s	8	elastic	none	no	no
L8_5s	8	elastic	none	no	yes
L12_1	12	pinned	none	2	no
L12_2t	12	elastic	none	2	no
L12_3	12	elastic	pinned	2	no
L12_4	12	elastic	pinned	2	yes
L12_5t	12	elastic	none	2	yes
L12_2s	12	elastic	none	no	no
L12_5s	12	elastic	none	no	yes

3.3.2 Geometry and Nodes

The OpenSees models represent three basic shear wall sizes: 4 *ft.* x 9 *ft.*, 8 *ft.* x 9 *ft.*, and 12 *ft.* x 9 *ft.* The physical configuration of a 4 *ft.* x 9 *ft.* shear wall is illustrated in Figure 17 and the node locations of the computation model are defined in Figure 18. The results of the computational models are compared to several shear wall tests performed at UNT (Liu et al., 2012).

(a) front view   (b) back view
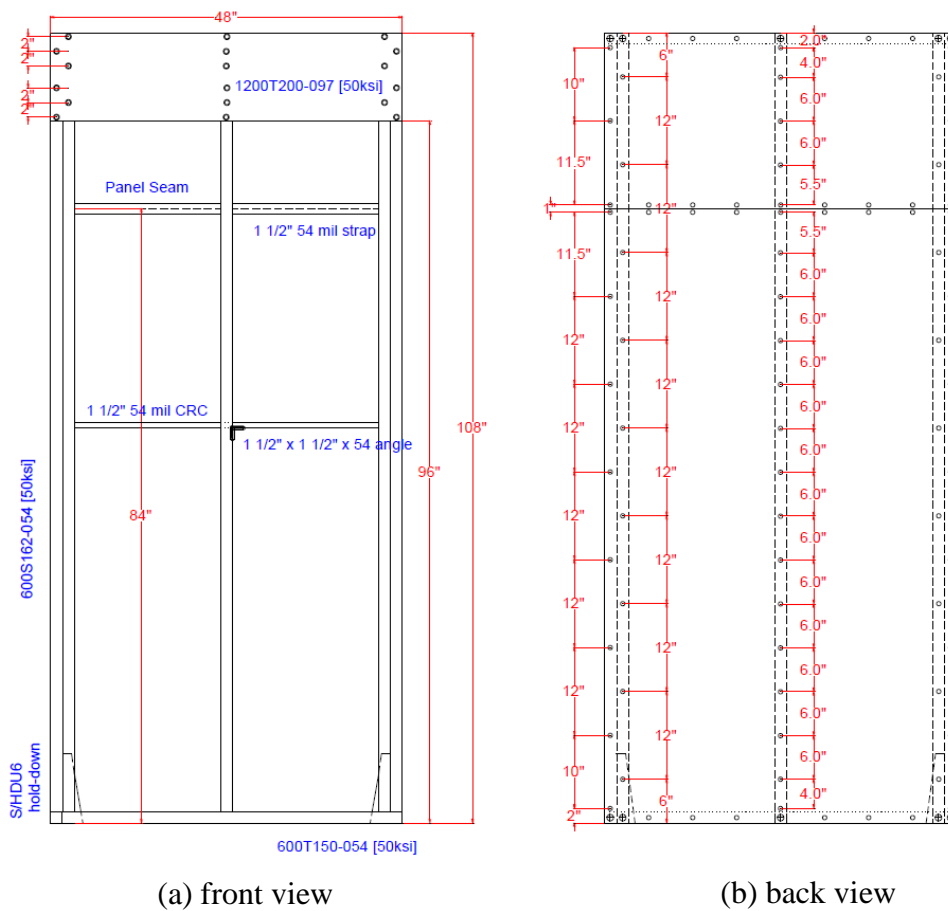
Figure 17. Geometry of 4 *ft.* x 9 *ft.* Physical CFS-OSB Shear Wall (Liu et al., 2012).
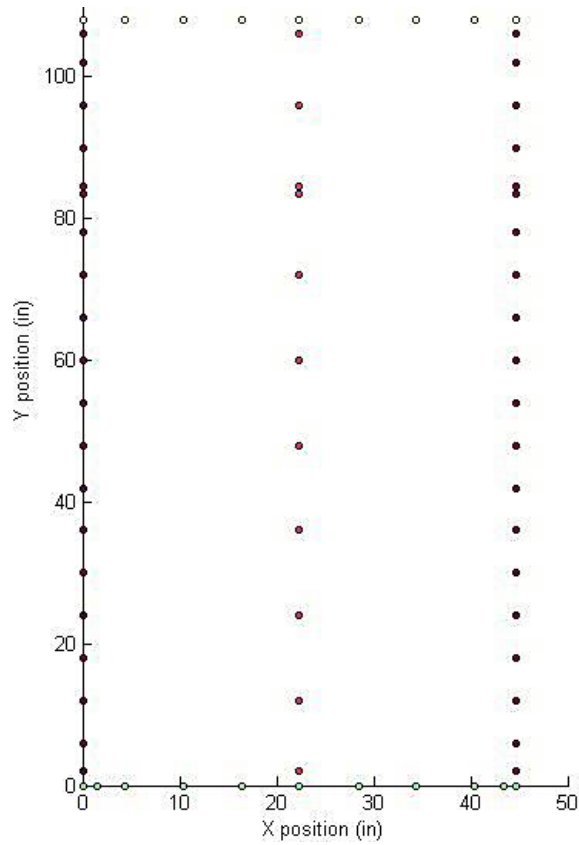
Figure 18. Nodes of a 4 *ft.* x 9 *ft.* OpenSees CFS-OSB Shear Wall Model.

3.3.3   CFS Studs and Tracks

The CFS tracks and studs were modeled using displacement-based beam elements (*dispBeamColumn* in OpenSees) with section properties given in Table 2 of Section 3.1. The steel framing members were subdivided with a node at each fastener location.

3.3.4 OSB Sheathing Panels

The OSB sheathing panels are modeled as rigid diaphragms, which include slave nodes at every fastener location and a master node at the center of the panel. The model does not incorporate the panel's shear stiffness.

3.3.5 Fastener Elements

Two coincident nodes were defined at each fastener location: one on the CFS frame members and another on the sheathing diaphragm. The fastener elements are one-dimensional, zero-length, radially symmetric elements (*CoupledZeroLength*). The uniaxial material properties assigned to the fastener elements are based on the results of physical testing of fasteners as described in Section 3.2. The radial stiffness of the fasteners is 12,205 *lb./in* (Peterman and Schafer, 2013). for linear analyses. For non-linear analyses, the fastener material is defined as a *Pinching4* material, which includes a multi-linear backbone curve and pinching (see Table 3 from Section 3.2.).

3.3.6 Ledger Track

The ledger track is modeled by creating a rigid diaphragm having the rectangular area equal to that of the web of the track. Since the ledger is directly connected to the studs in the physical model, the diaphragm in the computational model is also directly connected to the CFS frame nodes. As in the sheathing, the master node is again defined at the center of the rectangular area of the ledger. Although this does not account for the

deformation of the ledger track, the modeling is simpler than using a series of beam-column elements and rigid offsets to represent the ledger.

3.3.7 Stud-to-track Connections

The connections between vertical studs and top and bottom tracks were modeled as semi-rigid connections in rotation only. The nodes were connected by a rotational linear elastic spring and rigidly connected in translational degrees of freedom. Based on the measured lateral stiffness of the 4 *ft.* and 8 *ft.* bare CFS frames, the spring's rotational stiffness was estimated to be 100,000 *in-lb./rad*. This estimate was obtained by first analytically deriving the relationship between the stiffness of the CFS frame members and the rotational stiffness of stud-to-track connectors, and back-calculating the latter based on the measured stiffness of the UNT bare frame experiments (Liu et al., 2012).

3.3.8 Horizontal and Vertical Seams

CFS construction contains horizontal and vertical seams in the OSB sheathing: vertical seams are always supported by an interior stud and horizontal seams are bridged with a steel seam strap. In the OpenSees models, cases having no vertical seams (i.e. a single rigid diaphragm across the entire wall) and those having vertical seams spaced every 4 *ft.* (i.e. multiple dipahraghms) were investigated. A single diaphragm with no seams was the simpler computational model.

To models the shear walls with vertical seams, multiple rigid diaphragms, each of which is 4 *ft.* wide by 9 *ft.* tall, are created in OpenSees—thus the 8 *ft.* wide walls have two equal-width rigid diaphragms, and the 12 *ft.* walls have three. In the OpenSees models, the rigid diaphragms are allowed to slide past one another without interference. In actual construction the seam strap provide sufficient stiffness to prevent relative motion of the panels across the horizontal seam, and the strength of the seam strap sufficient to prevent its failure in typical applications. Preliminary study of models with horizontal seams revealed that additional modeling of steel straps would be necessary to restrain the large displacements which occur across a horizontal seam with no strap. Therefore, the computational models do not include the horizontal seam straps and instead use a single diaphragm across the vertical 9 *ft.* height.

3.3.9 Support Conditions

The physical tests include the hold-downs at the exterior chord studs, the bottom track includes additional nodes, offset 1.4375 *in.* from the centerline of the double stud to the position of the hold-down anchor bolt.

In the lateral translational direction, the hold-downs were modeled as fixed. In the rotational direction, the hold-downs were pinned. In the axial direction they were modeled as infinitely stiff (rigid) or by a uniaxial spring element. In the latter model, the tension stiffness of the hold-down was 56.7 *kips/in.* (Leng et al., 2013) and the compression stiffness was assigned a value of 1000 times greater than the tension stiffness in order to approximate bearing on a rigid foundation. The modeling of hold-

downs as a uniaxial spring element allows for non-linear analysis and is suitable for future cyclic tests. Shear anchors are not included in every OpenSees model but when they are present, they are modeled as fully pinned.

Details of the OpenSees model are summarized in the following Figure 19:
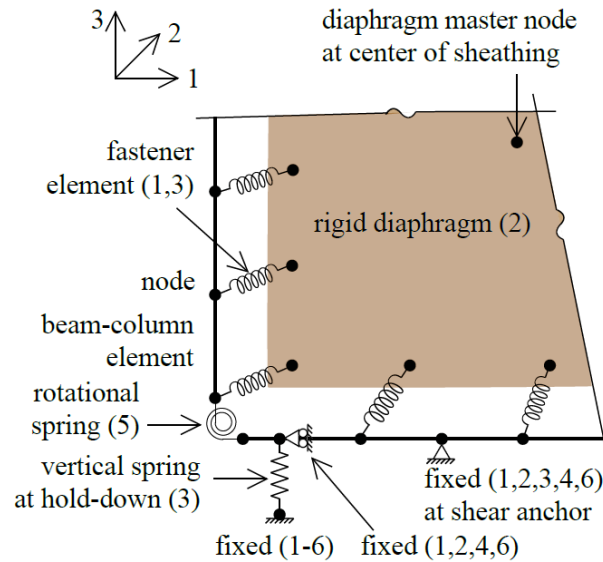

Figure 19. Details of OpenSees model: numbers in parentheses indicating active directions of spring elements or restrained directions of supports (Buonopane et al., 2014).

3.3.10 Loadings and Analysis Types

For all shear walls, the lateral pushover load of 1000 *lb.* is applied at the center node on the top track. This specific value of 1000 *lb.* is selected because this value was well within the linear range from University of Northern Texas physical testing results.

36

CHAPTER 4

4   RESULTS AND DISCUSSION

4.1   Linear Result Validations and Disucssion

The computational results are validated using three main methods:

(1) by drawing free-body diagrams of the shear wall panel and analyzing equilibrium at the support reactions,

(2) by employing equation C2.1-1 of AISI S213-07 and comparing the lateral deflections, and,

(3) by comparing computational results to experimental from University of Northern Texas.

In Table 5, the linear stiffnesses and displacements due to a 1000 *lb.* lateral force from all OpenSees models are shown.

Table 5. Stiffness and displacement from OpenSees linear analyses with applied 1000 _lb._ lateral force

Analysis Name	Stiffness (_lb._/_in._)	Displacement (_in._)	Comparison Test [#]
L4_1	14292	0.070	4
L4_2	5357	0.187	4
L4_3	9774	0.102	4
L4_4	11922	0.084	2
L4_5	5812	0.172	2
L8_1	32219	0.031	14
L8_2d	17714	0.057	14
L8_3	27462	0.036	14
L8_4	37188	0.027	12
L8_5d	20551	0.049	12
L8_2s	22214	0.045	14
L8_5s	24485	0.041	12
L12_1	48358	0.021	n/a
L12_2t	31757	0.032	n/a
L12_3	44953	0.022	n/a
L12_4	64007	0.016	n/a
L12_5t	38637	0.026	n/a
L12_2s	45497	0.022	n/a
L12_5s	52730	0.019	n/a

4.1.1 Model Validation Using Equilibrium

One approach to validate the simulation results from OpenSees is by sketching free-body diagrams of the panels, tracks and studs. In Figure 20, since the whole panel is in equilibrium, the moment created by applying the lateral force of 1,000 *lb.* should be equal to the moments caused by the reactions at hold-downs (or anchors). Also, the summation of horizontal forces at the supports (F_{x1} and F_{x2}) should be equal to 1,000 *lb.*, while the vertical forces should add up to zero.
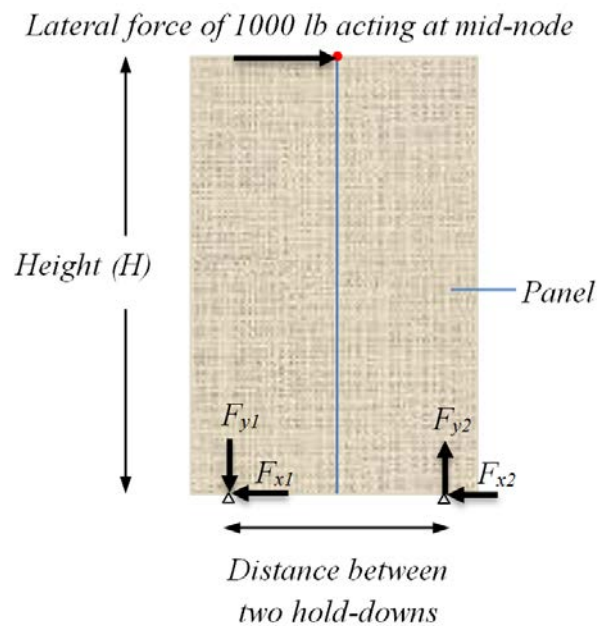

Figure 20. Free-body diagram of a 4 *ft.* wall panel.

Sample Calculation

For example, in linear analysis L4_1, the reactions are $F_{x1} = 500$ *lb.*, $F_{x2} = 499.92$ *lb.*, $F_{y1} = 2571$ *lb.* and $F_{y2} = 2571$ *lb.* Thus, the summation of all the vertical reactions is equal to zero, and the sum of the horizontal reaction forces at the two hold-downs are approximately equal to 1,000 *lb.* applied load. Since the distance between two hold-downs is 42 *in.*, the moment taken about the left hold-down due to F_{y2} is 107,982 *lb.-in*. This is approximately equal to moment created by the 1000 *lb.* lateral load (108,000 *lb.-in*). The small discrepancy between the two results is due to the nonlinear modeling of hold-downs as a uniaxial spring element.

OpenSees analyses also provide visualization of the entire shear wall (Figure 21). The blue and yellow panels represent OSB sheathing of the shear wall before and after the lateral load is applied, respectively. The original position of the framing studs and tracks are colored in red, and the displaced position in blue. Moreover, OpenSees can create graphical diagrams for the internal forces (axial, shear, moment) in the framing members as a result of force transfer at each individual fastener as shown in Figure 22a-f. At a minimum, the graphical diagrams reveal and validate the fundatmental relationships between axial, shear and moment diagrams.
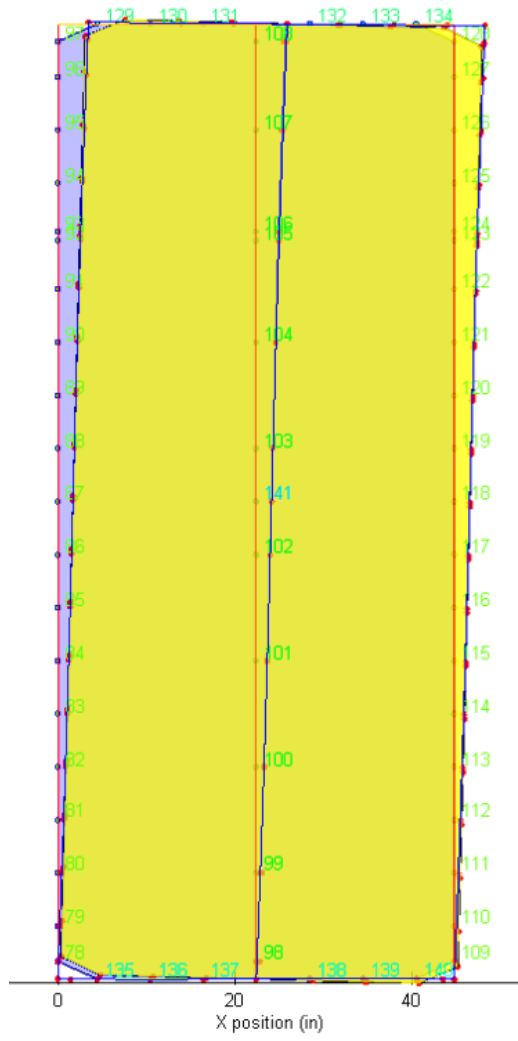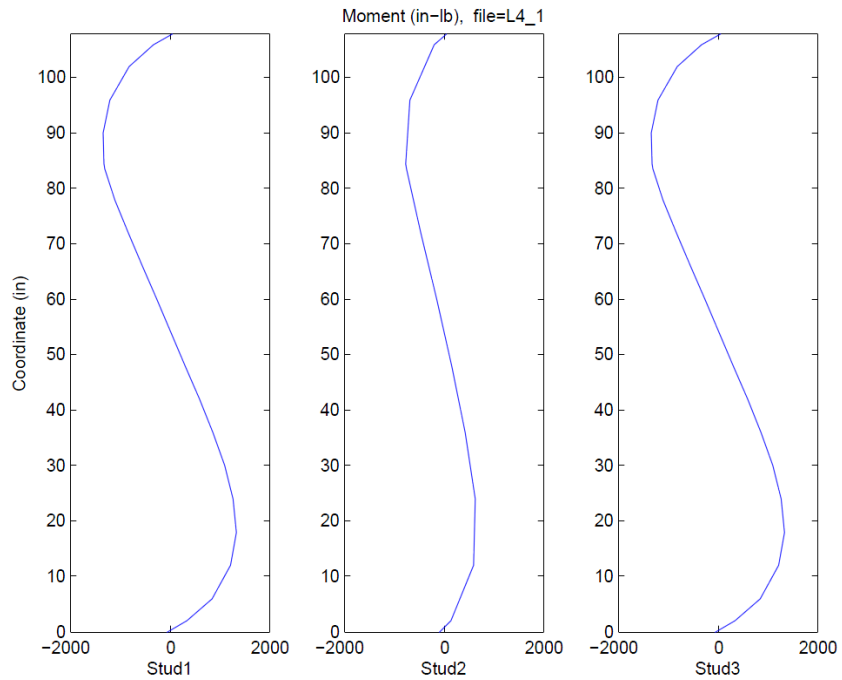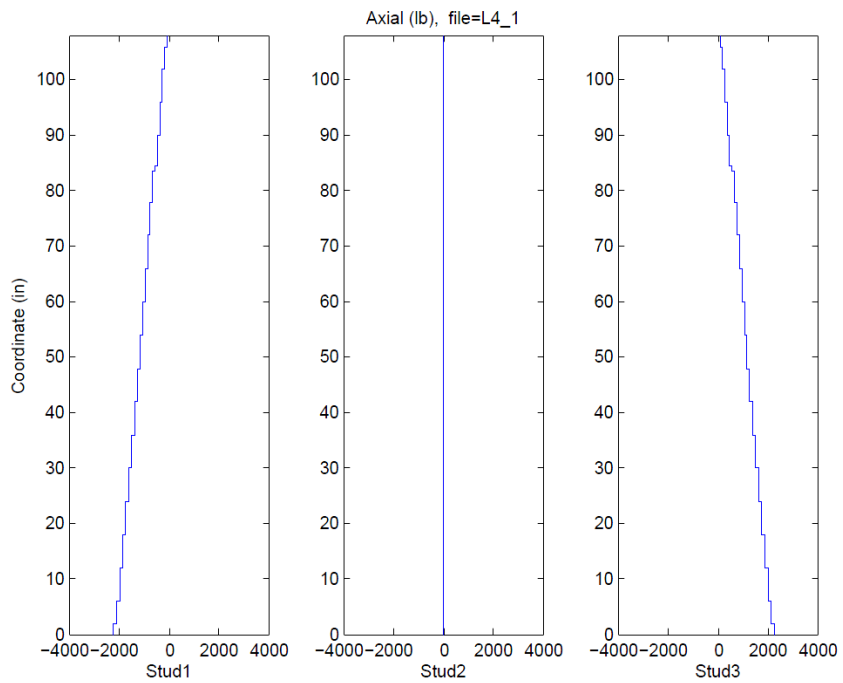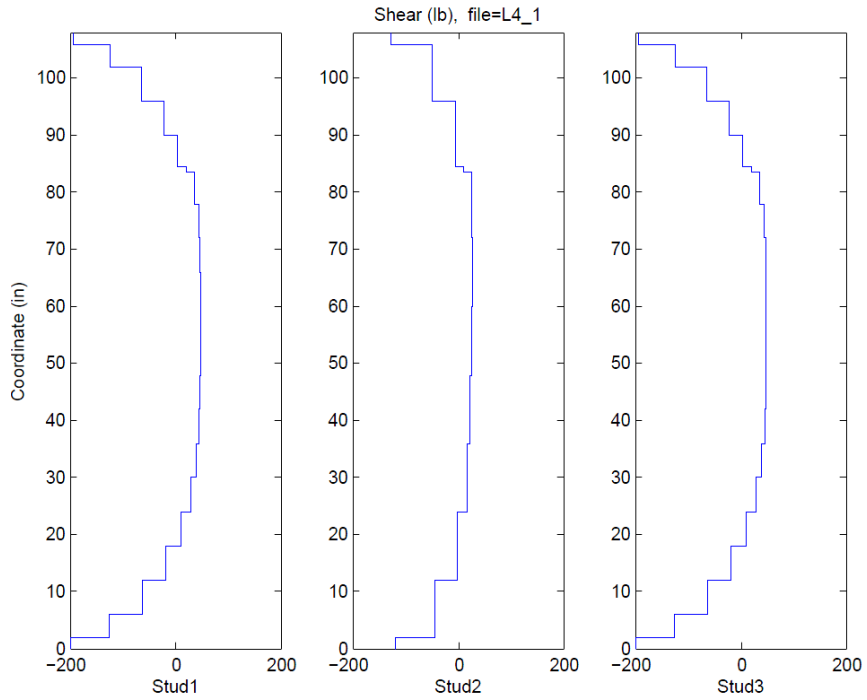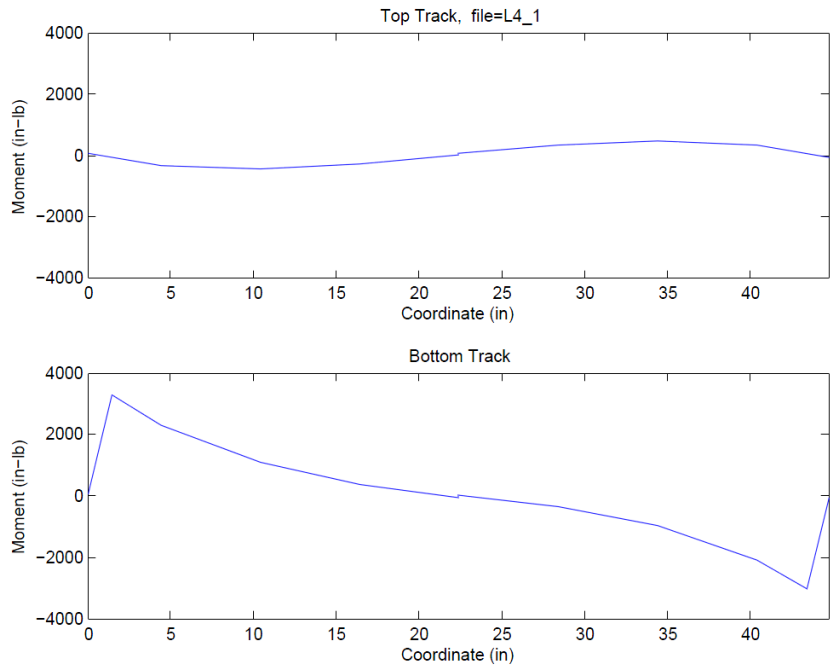
Figure 21. Visualization of model L4_1 at 1000 *lb*. lateral force.

(a)

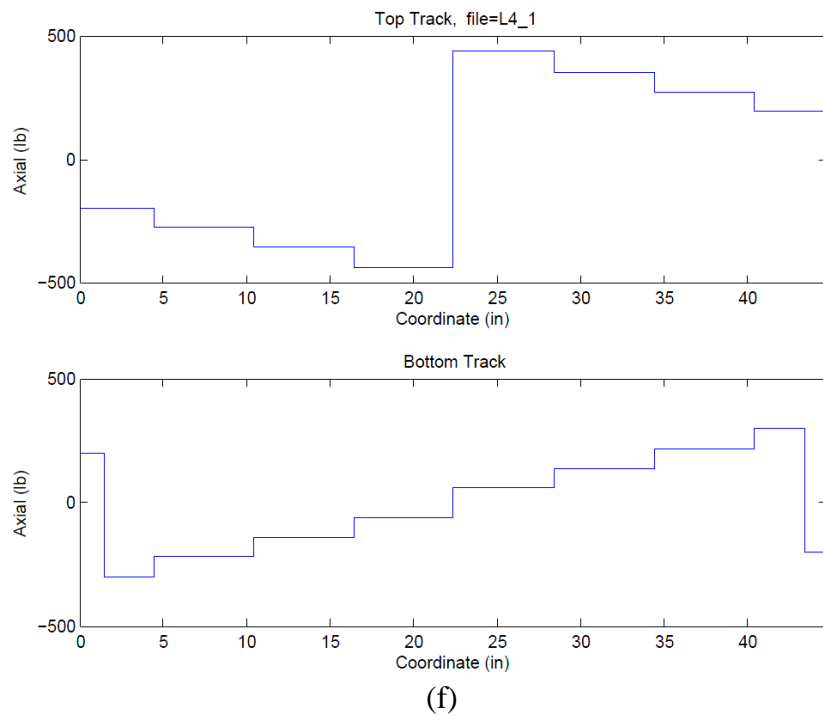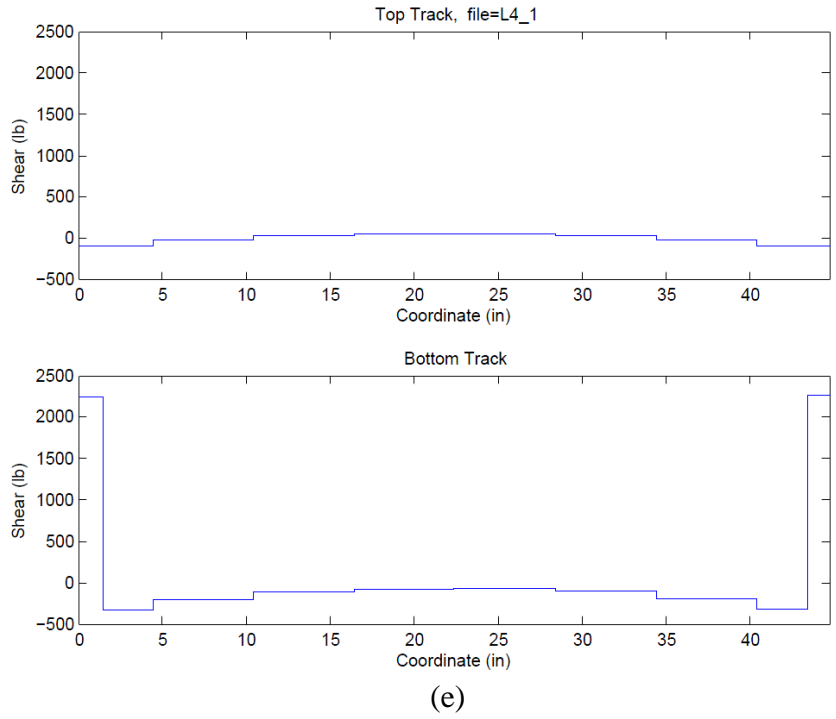(b)

(c)

(d)

(e)

(f)

Figure 22. Moment, axial and shear diagrams of: (a-c) vertical studs, (d-f) horizontal tracks.

4.1.2 Comparison to AISI S213 Equation

The lateral deflections estimated by OpenSees can be compared to those calculated using equation C2.1-1 of AISI S213-07. Table 6 provides deflection values and relative percentages of each contributing term at a lateral load of 1000 *lb.*, as well as at the design strength of the shear wall. The non-linear term and the hold-down term contribute substantially to the total deflection. As the applied load on the shear wall increases, the percent contribution from the non-linear term increases significantly, on the order of 70% to 80%.

Table 6. Values of displacements calculated from Eq. C2.1-1 of AISI 213-07

Width (ft)		Displacements at 1000 lb lateral force					Displacements at lateral strength						Strength (lbs)
		bending	shear	non-linear	hold-down	total	bending	shear	non-linear	hold-down	total		
4	(in)	0.011	0.017	0.093	0.089	0.210	0.033	0.050	0.798	0.262	1.142	(in)	2932
	%	5.28	8.04	44.17	42.50	100	2.86	4.34	69.89	22.92	100	%	
8	(in)	0.003	0.008	0.016	0.022	0.050	0.018	0.056	0.715	0.147	0.936	(in)	6600
	%	5.61	16.83	32.87	44.69	100	1.95	5.95	76.36	15.74	100	%	
12	(in)	0.001	0.006	0.006	0.010	0.023	0.012	0.056	0.584	0.098	0.750	(in)	9900
	%	5.29	24.67	26.43	43.61	100	1.63	7.43	77.86	13.10	100	%	

At a 1000 *lb.* lateral load, the total displacement using OpenSees models are 0.187 *in.* on the 4 *ft.* wall, 0.057 *in.* on the 8 *ft.* wall and 0.032 *in.* on the 12 *ft.* wall, respectively. These values are comparable to displacements at 1000 *lb.* lateral force estimated using C2.1-1. For the 4 *ft.* wall, the estimated lateral deflection due to the hold-downs from the computational model can be obtained by subtracting the displacements from L4_1 and L4_2, and is approximately 0.117 *in.* The S213 equation

predicts the lateral displacement to be 0.089 *in*. Similarly for the 8 *ft.* wall, the lateral deflection prediction from the S213 equation is 0.022 *in.* and from OpenSees 0.026 *in* (subtracting the lateral displacement of L8_1 from that of L8_2d). For the 12 *ft.* wall, the S213 lateral deflection is 0.010 *in.* and OpenSees deflection is 0.011 *in.* (subtracting the displacements from L12_1 and L12_2t). Thus, the two methods generally produce favorably comparable displacement results. It is important to note that these OpenSees models do not account for the sheathing shear flexibility. Therefore, the deflections from the computational model could be slightly increased by including the shear term from the S213 equation.

4.1.3   Comparison to Experimental Results

The linear analyses focus on examining the accuracy of four modeling features: hold-downs, shear anchors, vertical seams and ledger track (Table 4). The initial stiffnesses from OpenSees models are superimposed on the experimental results from University of Northern Texas (Liu et al., 2012).

By comparing the available experimental (Liu et al., 2012) and computational results of the 4 *ft.* and 8 *ft.* walls (L4_1 vs. L4_2 and L8_1 vs. L8_2d), it is observed that modeling of hold-down requires tension flexibility (Figure 23).
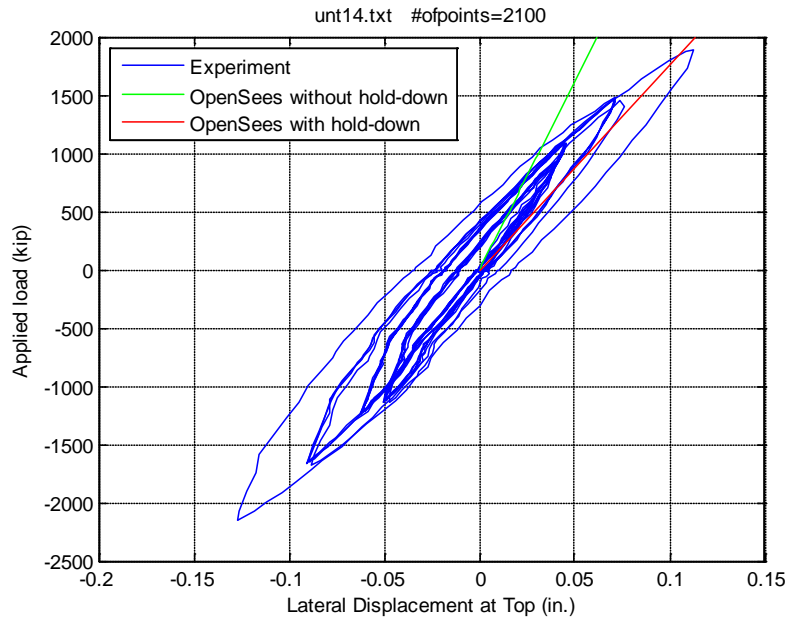
Figure 23. Effect of hold-downs on initial stiffness of 8 *ft.* wall model.

Modeling the shear anchors as fully-pinned connections produces lateral stiffness values which far exceed the UNT experimental results (Liu et al., 2012). Providing no support at the shear anchor locations produces lateral stiffnesses that more closely matched the experimental predictions (Table 5 and Figure 24).
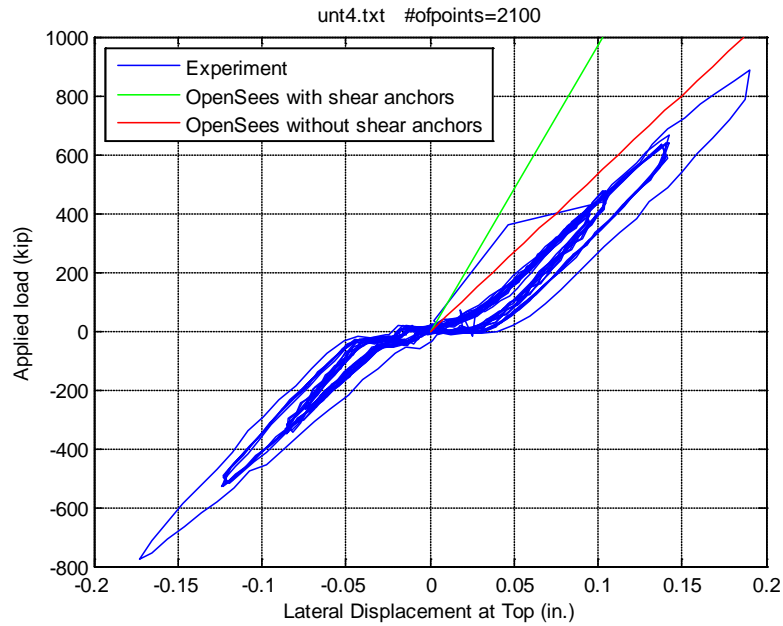
Figure 24. Effect of pinned shear anchors on initial stiffness of 4 *ft.* wall model.

The 8 *ft.* and 12 *ft.* walls provide a way to compare the effect of the presence of vertical seams in the computational model. The shear wall models with vertical seams create a decrease in lateral stiffness: approximately 25% for the 8 *ft.* wall (comparison between L8_2d and L8_2s) and 30% for the 12 *ft.* wall (comparison between L12_2t and L12_2s). In Figure 25, the OpenSees models are superimposed on the UNT experimental data (Liu et al., 2012). Based on this figure, both models have acceptable initial stiffnesses but in order to better reflect the physical model from UNT tests, models that incorporate vertical seams are selected for further non-linear studies.
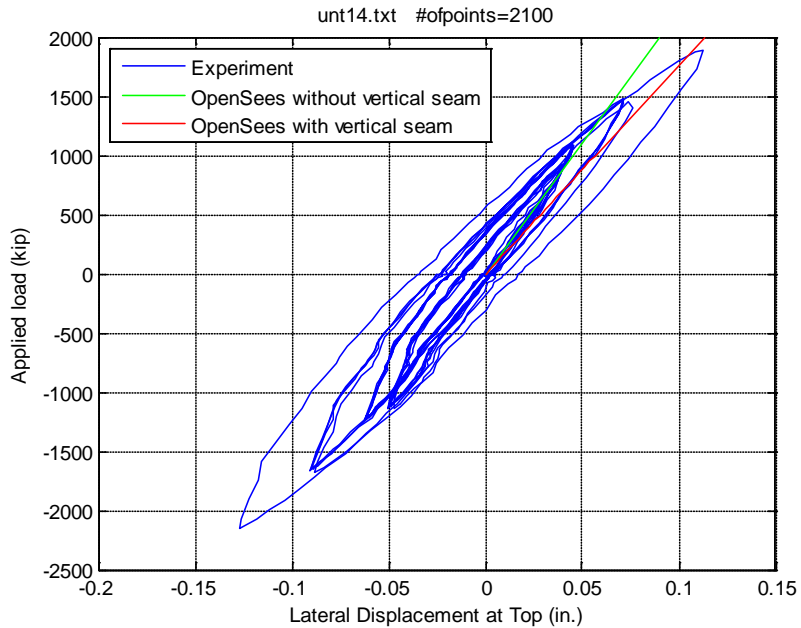
Figure 25. Effect of vertical seam on initial stiffness of 8 *ft.* wall model.

Including the ledger track in the OpenSees model results in an increase in lateral stiffness: about 8% for the 4 *ft.* wall (L4_2 vs. L4_5), 16% for the 8 *ft.* wall (L8_2d vs. L8_5d) and 20% for the 12 *ft.* wall (L12_2t vs. L12_5t). When the 4 *ft.* and 8 *ft.* wall OpenSees models are graphically compared to the experimental results, the effect of modeling the ledger track as a rigid diaphragm on initial stiffness is not very discernable (Figure 26 from Section 4.1.2).
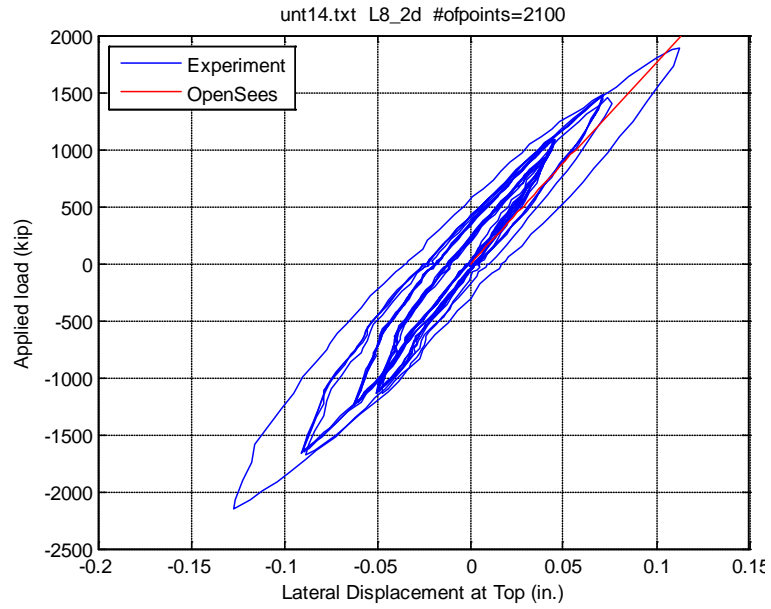
Based on all of the above results, a total of six models from linear analysis: L4_2, L4_5, L8_2d, L8_5d [Figure 26(a) to (d)], L12_2t and L12_5t are chosen for further non-linear analyses. The rest of the OpenSees linear analysis models can be found in the Appendix section.
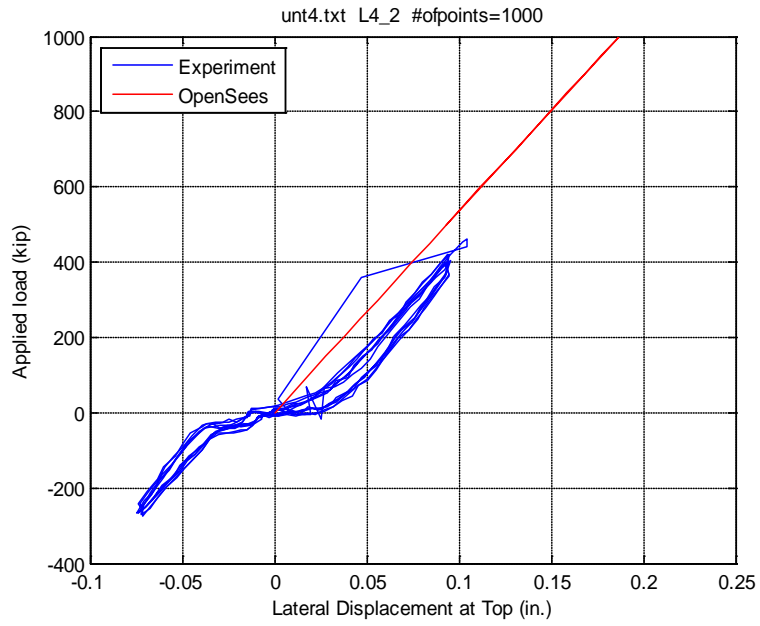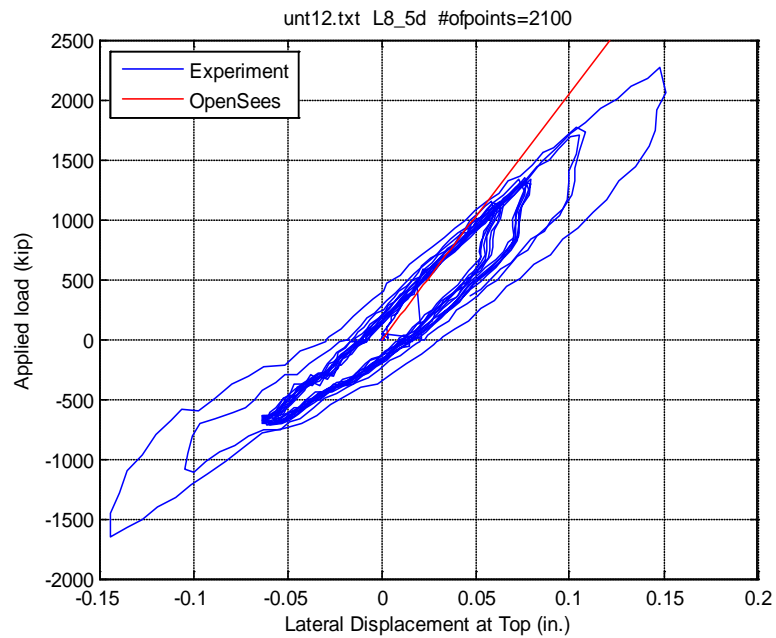
(a)
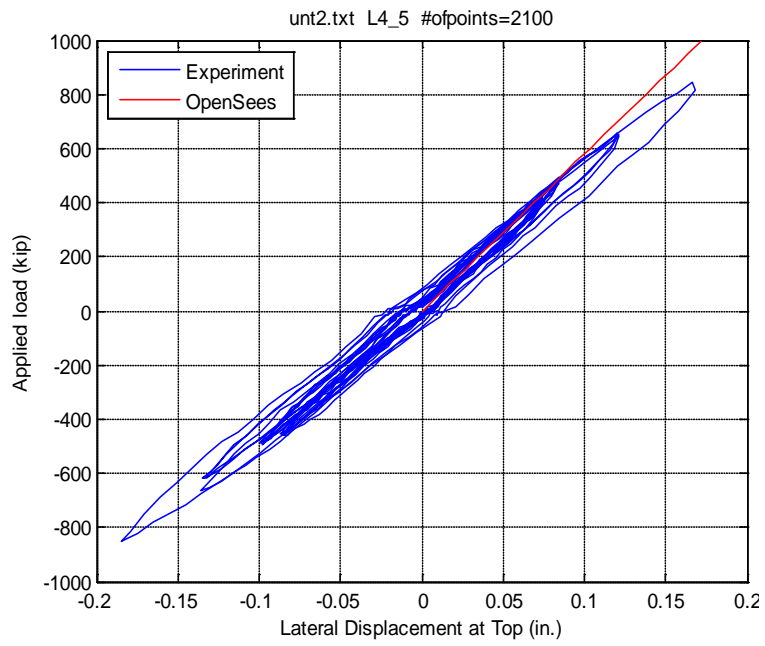
(b)

(c)

(d)

Figure 26. Chosen linear models with OpenSees initial stiffness graphs (red) superimposed on the UNT experimental data (Liu et al., 2012) (blue) : (a) L4_2, (b) L4_5, (c) L8_2d, (d) L8_5d.

4.2 Summary and discussion of results from non-linear analysis

For the non-linear analyses, the OpenSees models use the *Pinching4* material model defined with the parameters, as described in Section 3.2. Using monotonic displacement control, the models were loaded until the peak load was achieved. The peak loads along with the lateral displacement at this load for each model are provided in Table 7.

Table 7. Summary of non-linear analyses results from OpenSees models

Width (ft)	Computational Results			Experimental Results		
	Analysis Name	Max. Load (lbs)	Displacement at max. load (in)	Comparison Test (Liu et al., 2012)	Max. Load (lbs)	Displacement at max. load (in)
4	NL4_2	4078	1.872	4	4016	2.400
	NL4_5	6024	1.852	2	4408	2.815
8	NL8_2d	8315	1.538	14	8710	1.938
	NL8_5d	11522	1.376	12	9246	1.964
12	NL12_2t	12560	1.446	n/a	--	--
	NL12_5t	16871	1.220	n/a	--	--

The estimated displacements from OpenSees at maximum load are smaller than the corresponding experimental values. On the other hand, the computational models without including the ledger (NL4_2 and NL8_2d) more closely predict the experimental peak load in non-linear analyses than those with ledgers (NL4_5 and NL8_5d). Models with the ledger represented as a rigid diaphragm result in maximum strengths significantly greater than the experimental strengths. Hence, modeling the ledger as a rigid diaphragm is not appropriate beyond small lateral loads.

Figure 27 compares the OpenSees load-deflection response with the experimental cyclic test results of the 8 *ft.* shear wall. As seen in the diagram, the computational model predicts the strength and bounding backbone curve from the cyclic tests well even though it unloads one peak earlier. Other non-linear OpenSees results are shown in Figure 28.
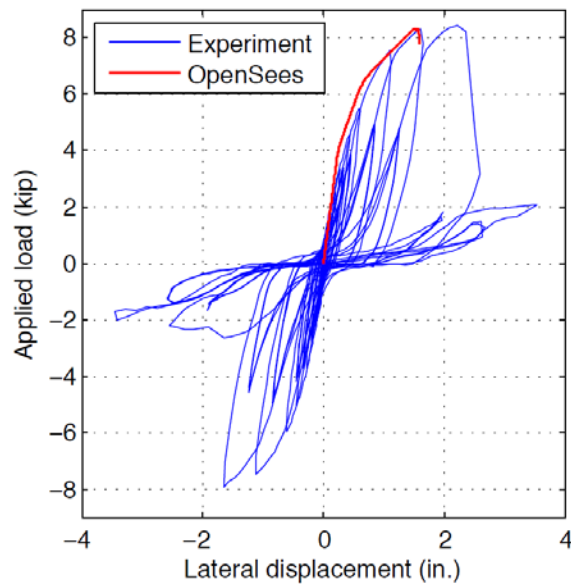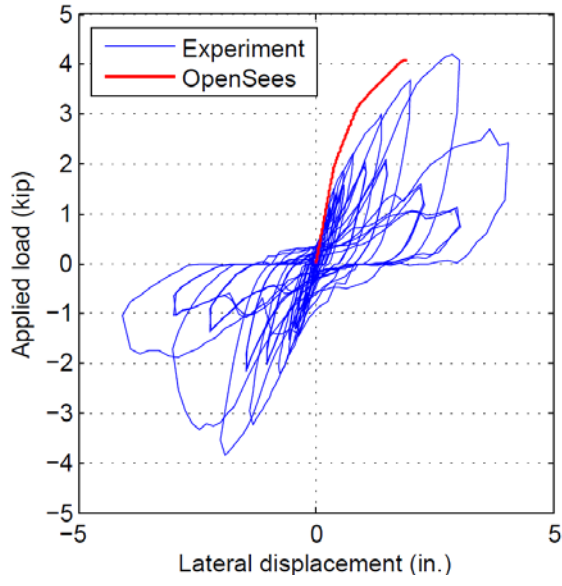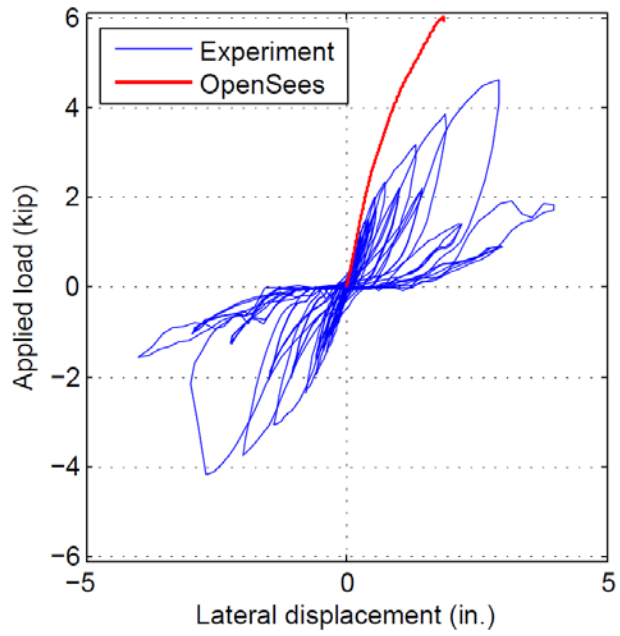

Figure 27. Non-linear response of model NL8_2d on test 14 of Liu et al. (2012).
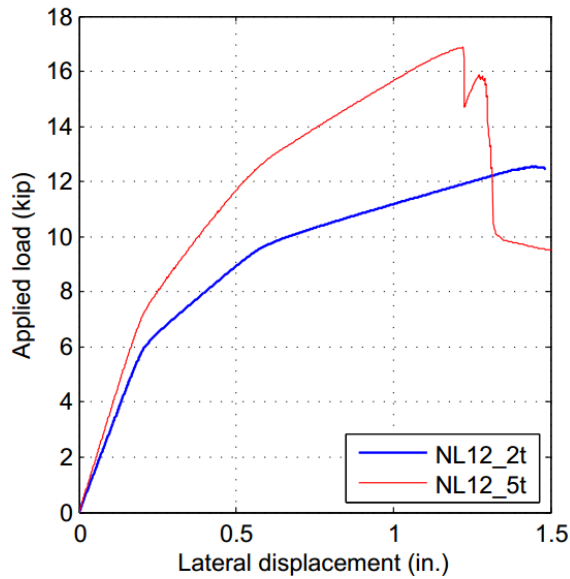
(a)

(b)

54
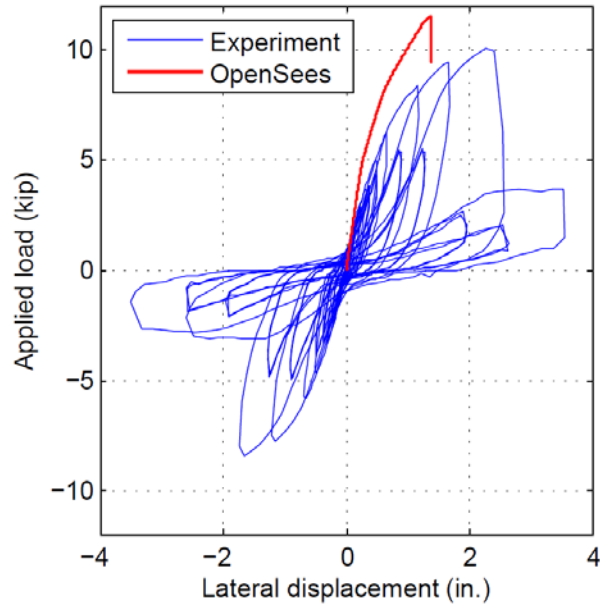
(c)

(d)

Figure 28. OpenSees non-linear responses: (a) model NL4_2 superimposed on UNT test 4 of Peterman and Schafer (2013), (b) model NL4_5 superimposed on UNT test 2 of Peterman and Schafer (2013), (c) model NL8_5d superimposed on UNT test 12 of Peterman and Schafer (2013), (d) models NL12_2t and NL12_5t (no experimental data available).

Modeling the individual fasteners permits a more detailed examination of the interaction forces between the fasteners, the framing members and the sheathing than is possible in typical experiments. A vector plot of the 8 *ft.* shear wall (NL8_2d) shows the magnitude and direction of each fastener force at the lateral strength (Figure 29a).

While the design assumption would usually suppose vertical uniform force transfer, the vector plot reveals that forces are not only non-vertical but also the magnitudes (the lengths of the vector force) vary across the shear wall. The diagonal forces near the bottom corners of the vector plot reflect the observed experimental behavior of fasteners near the corner of the shear wall causing sufficient damage to the sheathing OSB to pull through (Figure 29b).
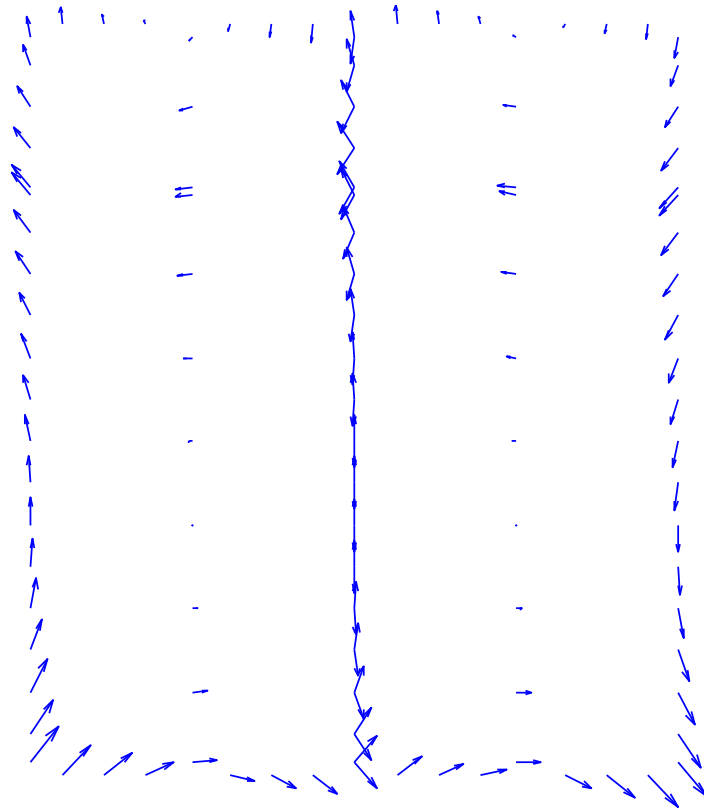
(a)   (b)

Figure 29. (a) Vector plot of fastener force at peak strength for model NL8_2d (Buonopane et al., 2014), (b) An example of observed fastener pull-through failure at the bottom corner which can be predicted by fastener force vector plot (Liu et al., 2012).

4.3   Preliminary Study of 4 *ft.* x 9 *ft.* Wall with Corner Detail

The fastener-based OpenSees modeling technique can be extended to other Wall configurations. At the University at Buffalo in New York, a two-story CFS building was fabricated to study seismic response of the structure (Madsen et al., 2011). Compared to previous models (especially to L4_2), where both hold-downs are inside the wall, the right hold-down in this model is outside of the chord stud (Figure 30). Since this particular shear wall is connected to another wall at the building corner, an additional corner stud is inserted and the outermost hold-down is repositioned 6 *in.* to the right.
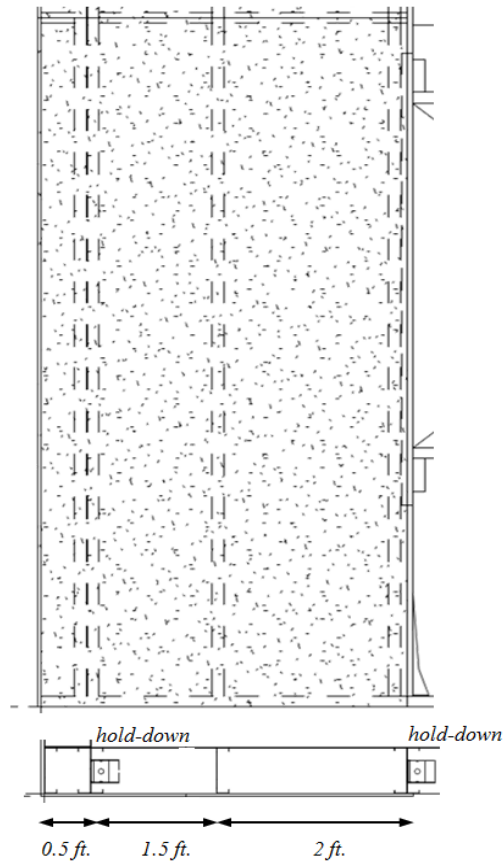

Figure 30. The elevation and plan view of a 4 ft. x 9 ft. wall of a two-story steel building (Madsen et al., 2011).

Four models were created to study how the construction details at the corner affect the response of the shear wall (Table 8). Model L4_2 is the baseline 4 *ft.* wall model with features detailed in Table 4 of Section 3.3.1. While the baseline model has both hold-downs inside the shear wall, the other models (L4_h2, L4_h2a, L4_h2b, L4_h2c) have hold-downs positioned according to the construction of the test structure at University of Buffalo. Additional corner stud is included in models L4_h2a, L4_h2b and L4_h2c, which incorporate various fastener spacings as seen in the following table.

Table 8. OpenSees model variations for the corner 4 *ft.* x 9 *ft.* wall

Model Name	Model Features			Stiffness (*lb./in.*)	Displacement (*in.*)
	account for corner stud	corner stud fastener spacing (*in.*)	Fastener spacing for stud near the left hold-down (*in.*)		
L4_2	no	n/a	6	5357	0.1870
L4_h2	no	n/a	6	5088	0.1966
L4_h2a	yes	6	12	5105	0.1959
L4_h2b	yes	12	6	5149	0.1942
L4_h2c	yes	6	6	5209	0.1920

The initial stiffness value of L4_h2 is smaller than that of L4_2 model. And, the stiffness values of L4_h2a, L4_h2b and L4_h2c are close to L4_h2. Based on the following vector plots (Figure 31), there are force transfers in both the corner stud and its adjacent chord stud. These vector plots suggest that the shear wall models cannot ignore the presence of the additional corner stud and simply assume a 3.5 *ft.* wide shear

wall. Thus, the future work would be to model a 3.5 *ft.* shear wall and compare its initial

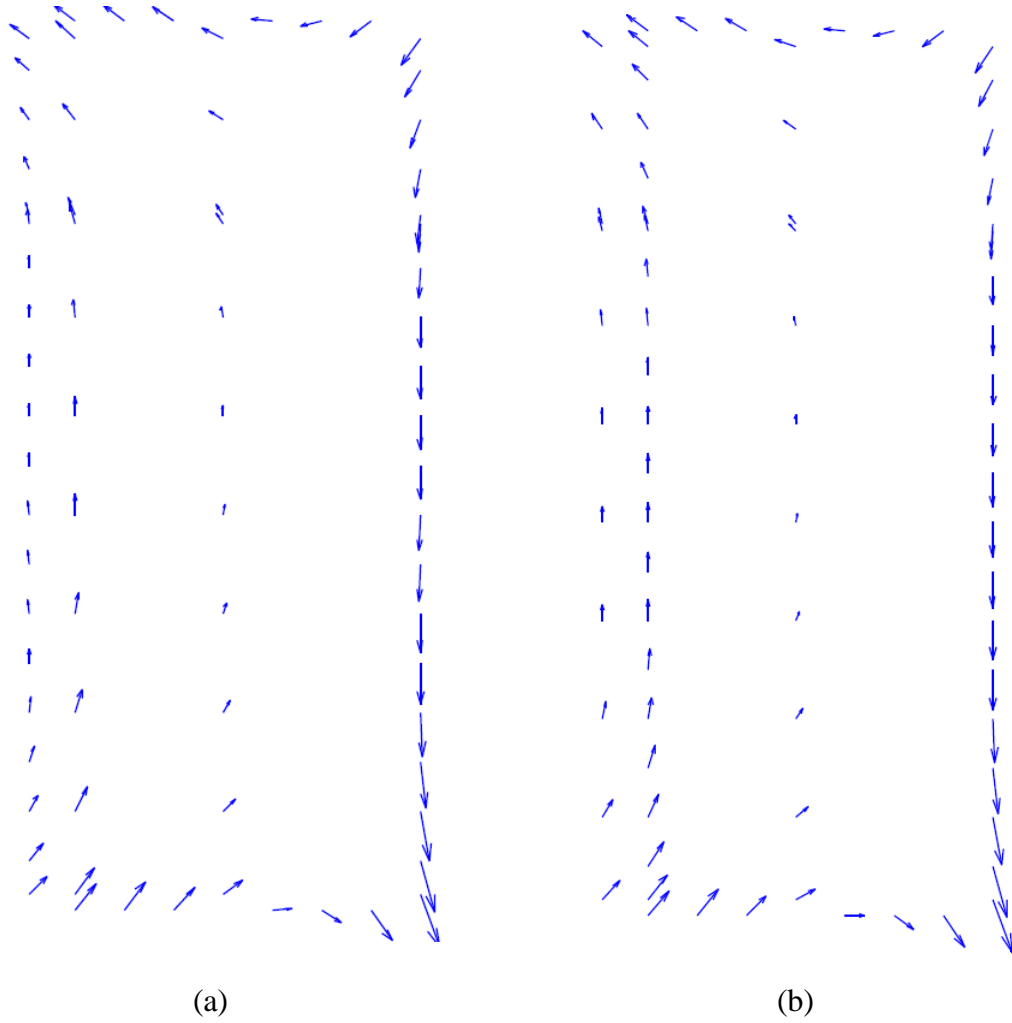stiffness to those given in Table 8.

(a)   (b)

Figure 31. Vector plots of modified 4 *ft.* wall: (a) L4_h2a, (b) L4_h2b.

CHAPTER 5

5   CONCLUSIONS AND FUTURE WORK

The objective of this research was to develop and validate fastener-based models of CFS shear walls using the OpenSees structural analysis software. The ability to accurately predict initial stiffness, lateral strength and non-linear behavior of the shear walls is important for the performance-based seismic design of CFS structures. The research approach was based on the understanding that the complex interaction of the fasteners with the sheathing plays a significant role in the non-linear behavior of the CFS shear walls.

The OpenSees models developed for this research used beam-column elements for the framing members and a rigid diaphragm for the OSB sheathing panel. Each individual fastener that connects the framing members and the sheathing was modeled as a radially symmetric linear or non-linear spring element. The modeling parameters for the fasteners are obtained from fastener tests. For the non-linear analyses, the *Pinching4* material model in OpenSees was employed. The *Pinching4* element allows for non-linear loading and unloading, pinching and deterioration of strength and stiffness. To model fastener elements, results from Johns Hopkins University (JHU) were employed.

Shear walls of widths 4 *ft.*, 8 *ft.* and 12 *ft.* were modeled in OpenSees to study the effects of four specific features—hold-downs, shear anchors, panel seams and ledger track—on the initial stiffness and strength of the CFS shear walls. In addition, a study of

a 4 *ft.* wide wall with various corner details was performed. The results were validated using three methods: (1) external equilibrium and internal force diagrams, (2) comparison of lateral deflections to those predicted from empirically derived equations in the seismic design code (AISI S213-07 2007), and (3) comparison to University of Texas (UNT) full-scale test results of 4 *ft.* and 8 *ft.* walls.

Overall, in the OpenSees models, hold-downs with tension flexibility were needed to better represent the initial stiffness of the physical testings. Models with vertical panel seams closely predicted the initial stiffnesses of the experimental results. Presence of fully rigid shear anchors resulted in overestimation of the lateral stiffnesses. Modeling the web of the ledger track as a rigid diaphragm slightly increased the initial stiffness of the shear wall, but the non-linear strength significantly exceeded the experimental results. Modeling every individual fastener allows close examination of the interaction forces between the fasteners, framing members and sheathing. Vector plots of the fastener forces allow visualization of the complex force interaction. The significance of this research, thus, is the development of computational tools which have the ability to accurately model the non-linear response with various specific construction details without the need for performing full scale testing.

For future work, the ledger track could be modeled using beam elements and rigid offsets. OpenSees models could also include horizontal seams but at these seams steel straps would need to be incorporated. In addition, modeling of shear anchors could be done with stiffness properties based on physical testing results. Future work should also

seek to adjust the non-linear OpenSees model to be more reflective of the experimental deflections. One way to achieve is this by studying the effect of the Pinching4 fastener model parameters related to unloading and degradation on the global wall displacements.

Further development of this research potentially includes full non-linear cyclic analysis, application of gravity loads and seismic excitation. Finally, the fastener-based computational approach can be employed to model in-plane stiffness of floor diaphragms and to examine the load sharing between shear and gravity walls.

BIBLIOGRAPHY

ASTM E564 (2006). "Standard Practice for Static Load Test for Shear Resistance of Framed Walls for Buildings," ASTM International, West Conshohocken, PA, 2006, DOI: 10.1520/E0564-06, www.astm.org.

AISI-S100-07 (2007). "North American Specification for the Design of Cold-Formed Steel Structural Members," American Iron and Steel Institute, Washington, D.C., AISI-S100-07.

AISI-S200-07 (2007). North American Standard for Cold-Formed Steel Framing – General Provisions. American Iron and Steel Institute, Washington, D.C., AISI-S200-07.

AISI-S213-07 (2007). North American Standard for Cold-Formed Steel Framing– Lateral Design. American Iron and Steel Institute, Washington, D.C., AISI-S213-07.

Buonopane S. G., T. H. Tun, and B. W. Schafer (2014). "Fastener-based computational models for prediction of seismic behavior of CFS shear walls," in *Tenth U.S. National Conference on Earthquake Engineering*, Anchorage, Alaska, 2014.

Celik, K., Engleder, T. (2010). Shear walls with cold-formed steel framing and wood structural panel sheathing. Conference Proceedings of International Symposium

"Steel structures: Cultural & Sustainability 2010". Istanbul, September 21-23, 2010.

Della Corte G, Fiorino L, Landolfo R. (2006). "Seismic behavior of sheathed cold-formed structures: numerical study," *Journal of Structural Engineering* 2006; 132(4):558-569.

Filiatrault, A. (1990). "Static and dynamic analysis of timber shear walls," Can. J. Civ. Engrg., Ottawa, 17(4), 643–651.

Filiatrault, A., and Folz, B. (2004a). "Seismic analysis of woodframe structures. I: Model implementation and formulation," *Journal of Structural Engineering*. Vol. 130: 9, 1353-1360.

Filiatrault, A., and Folz, B. (2004b). "Seismic analysis of woodframe structures. II: Model implementation and verification," ASCE Journal of Structural Engineering. Vol. 130: 9, 1361-1370.

Fiorino, L., G. D. Corte, Landolfo R. (2006). "Lateral response of sheathed cold-formed shear walls: an analytical approach," *Eighteenth International Specialty Conference on Cold-Formed Steel Structures*. Orlando, Florida, USA, October 26-27, 2006.

Fiorino, L., O. Iuorio, R. Landolfo. (2012). "Seismic analysis of sheathing-braced cold-formed steel structures," Engineering Structures (Elsevier Science) 2012; 34:538-547.

Folz B, Filiatrault A. (2001). "Cyclic analysis of wood shear walls," *Journal of Structural Engineering* 2001; 127(4): 433-441.

Fülöp LA, Dubina D (2004). "Performance of wall-stud cold-formed shear panels under monotonic and cyclic loading. Part II: Numerical modelling and performance analysis," *Thin-Walled Structures* 2004; 42: 339-349.

K.D. Peterman, B.W. Schafer (2013). "Hysteretic shear response of fasteners connecting sheathing to cold-formed steel studs" Research Report, CFS-NEES, RR04, January 2013, access at www.ce.jhu.edu/cfsnees.

Leng, J., Schafer, B.W., Buonopane, S.G. (2013). "Modeling the seismic response of cold-formed steel framed buildings: model development for the CFS-NEES building." Proceedings of the Annual Stability Conference - Structural Stability Research Council, St. Louis, Missouri, April 16-20, 2013, 17pp.

Lowes, L., Mitra, N., Altoontash, A (2004). A Beam-Column Joint Model for Simulating the Earthquake Response of Reinforced Concrete Frames. PEER Report 2003/10, www.peer.berkeley.edu.

McKenna F. OpenSees: The Open System for Earthquake Engineering Simulation. http://opensees.berkeley.edu.

P. Liu, K.D. Peterman, B.W. Schafer (2012). "Test Report on Cold-Formed Steel Shear Walls" Research Report, CFS-NEES, RR03, June 2012, access at www.ce.jhu.edu/cfsnees.

R.L. Madsen, N. Nakata, B.W. Schafer (2011). "CFS-NEES Building Structural Design Narrative", Research Report, RR01, access at www.ce.jhu.edu/cfsness, October 2011, revised 2013.

Serrette R, Chau K., (2003). "Estimating the response of cold-formed steel frame shear walls," AISI *Research Report RP03-7*; 2003.

Serrette R. L, Hall G, Nygen J, (1996). "Shear wall values for light weight steel framing," USA: AISI, 1996.

Serrette, R.L. (1997). "Additional Shear Wall Values for Light Weight Steel Framing," Final Report, Santa Clara University, Santa Clara, CA, 1997.

Serrette, R.L. (2002). "Performance of Cold-Formed Steel-Framed Shear Walls: Alternative Configurations," Final Report: LGSRG-06-02, Santa Clara University, Santa Clara, CA, 2002.

Xu L, Martínez J. (2006). "Strength and stiffness determination of shear wall panels in cold-formed steel framing," *Thin-Walled Structures* 2006; 44: 1084-1095.

APPENDIX
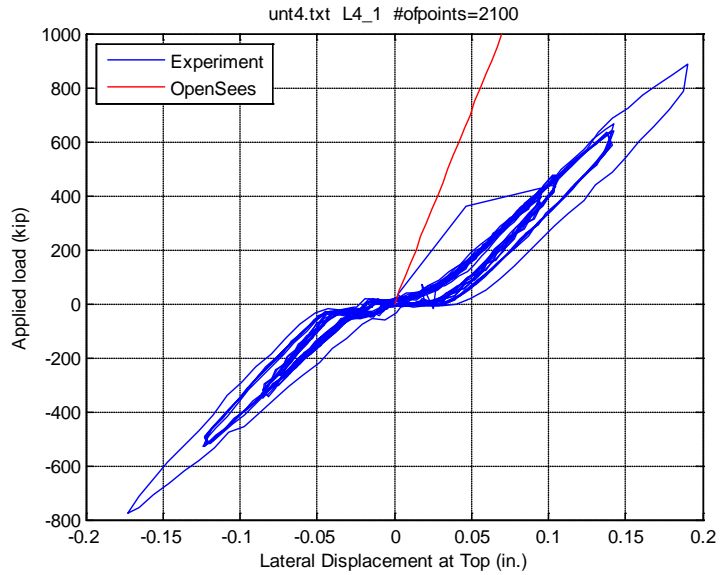
Figure A.1. Linear stiffness of model L4_1 superimposed on UNT test 4 (Peterman and Schafer, 2013).
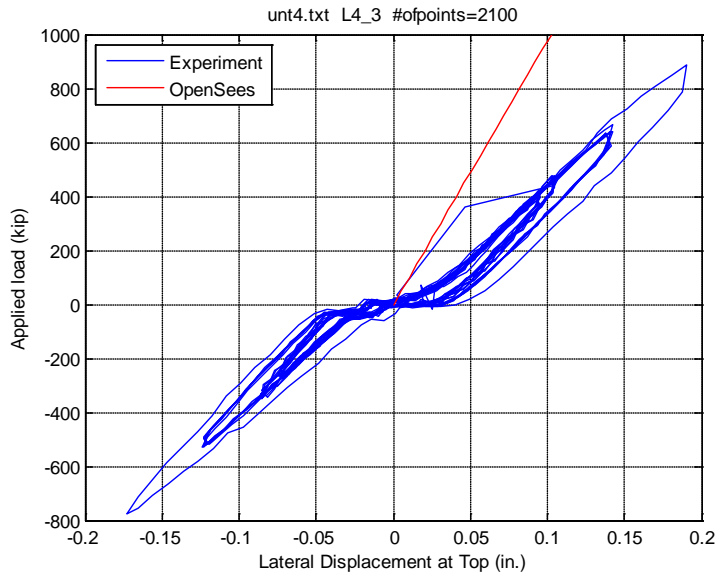

Figure A.2. Linear stiffness of model L4_3 superimposed on UNT test 4 (Peterman and Schafer, 2013).
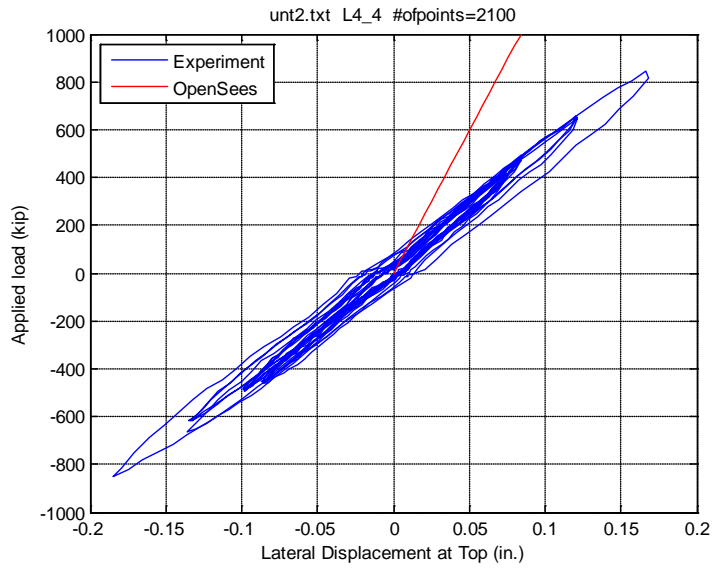
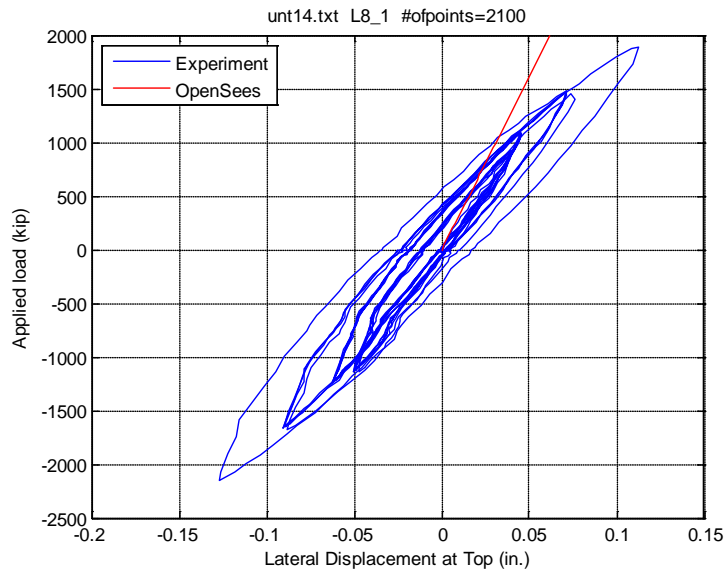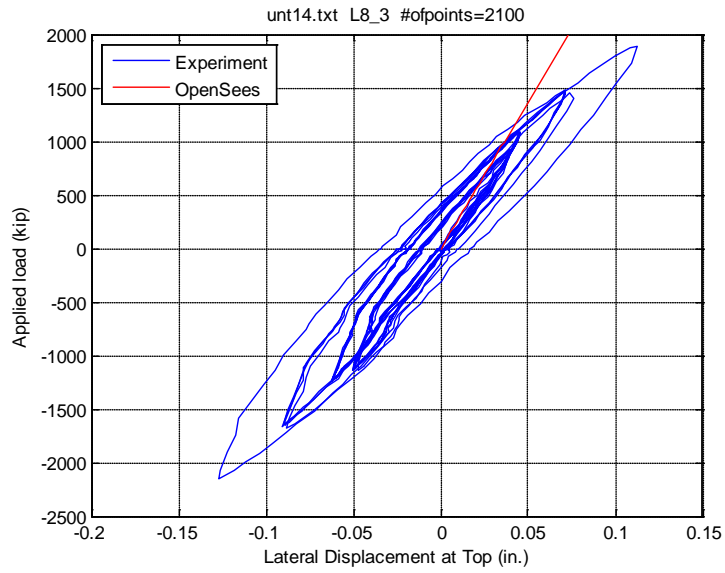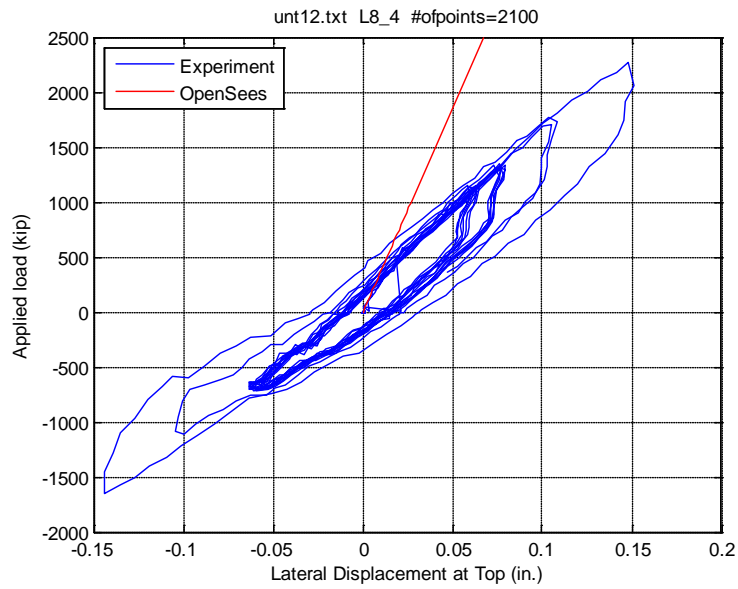**Figure A.3. Linear stiffness of model L4_4 superimposed on UNT test 2 (Peterman and Schafer, 2013).**

Figure A.4. Linear stiffness of model L8_1 superimposed on UNT test 14 (Peterman and Schafer, 2013).

Figure A.5. Linear stiffness of model L8_3 superimposed on UNT test 14 (Peterman and Schafer, 2013).

Figure A.6. Linear stiffness of model L8_4 superimposed on UNT test 12 (Peterman and Schafer, 2013).
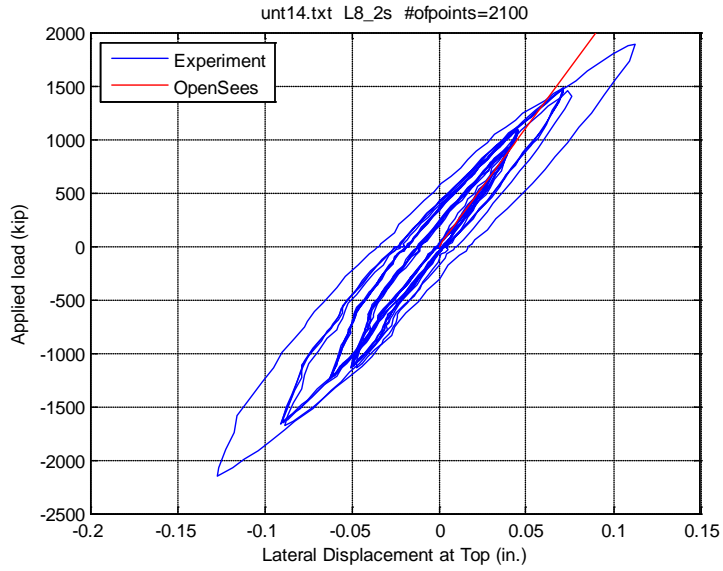
Figure A7. Linear stiffness of model L8_2s superimposed on UNT test 14 (Peterman and Schafer, 2013).
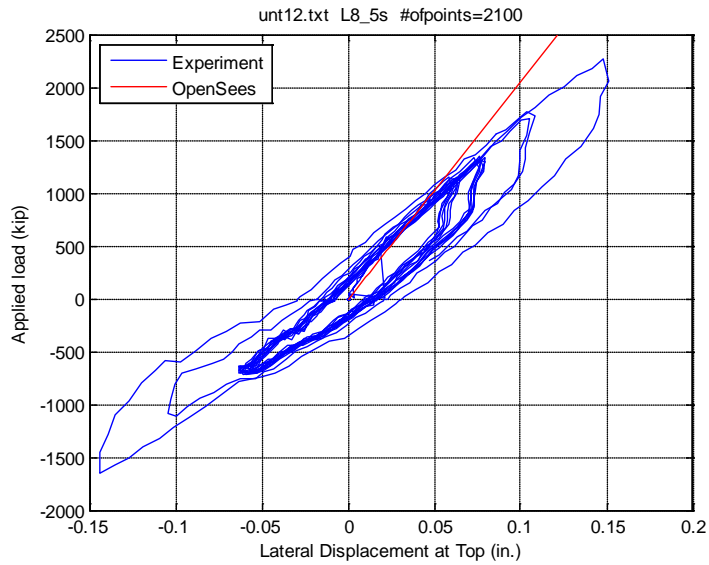

Figure A8. Linear stiffness of model L8_5s superimposed on UNT test 12 (Peterman and Schafer, 2013).